



Squeezing atmospheric muons

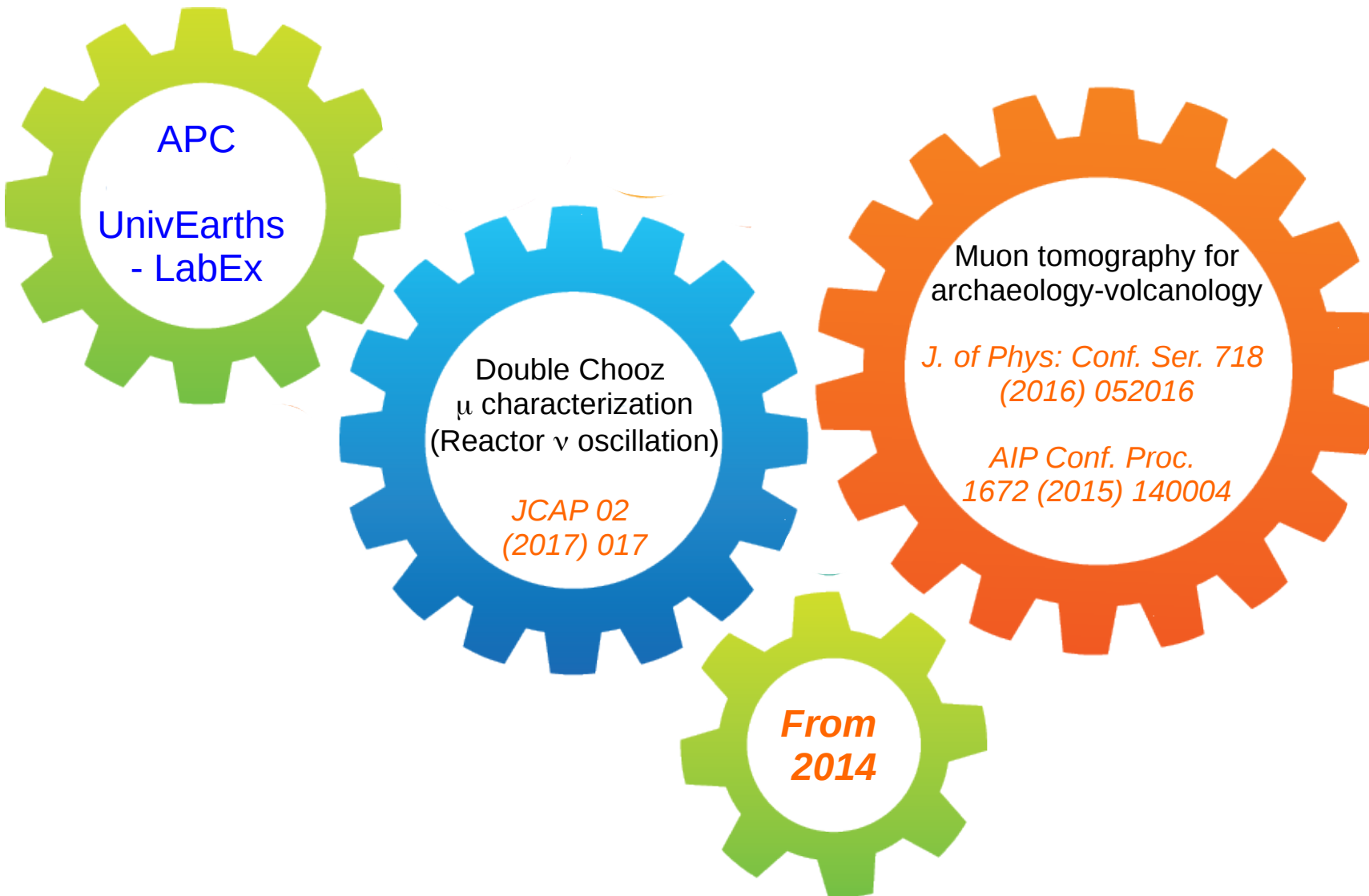
From neutrino physics to imaging applications

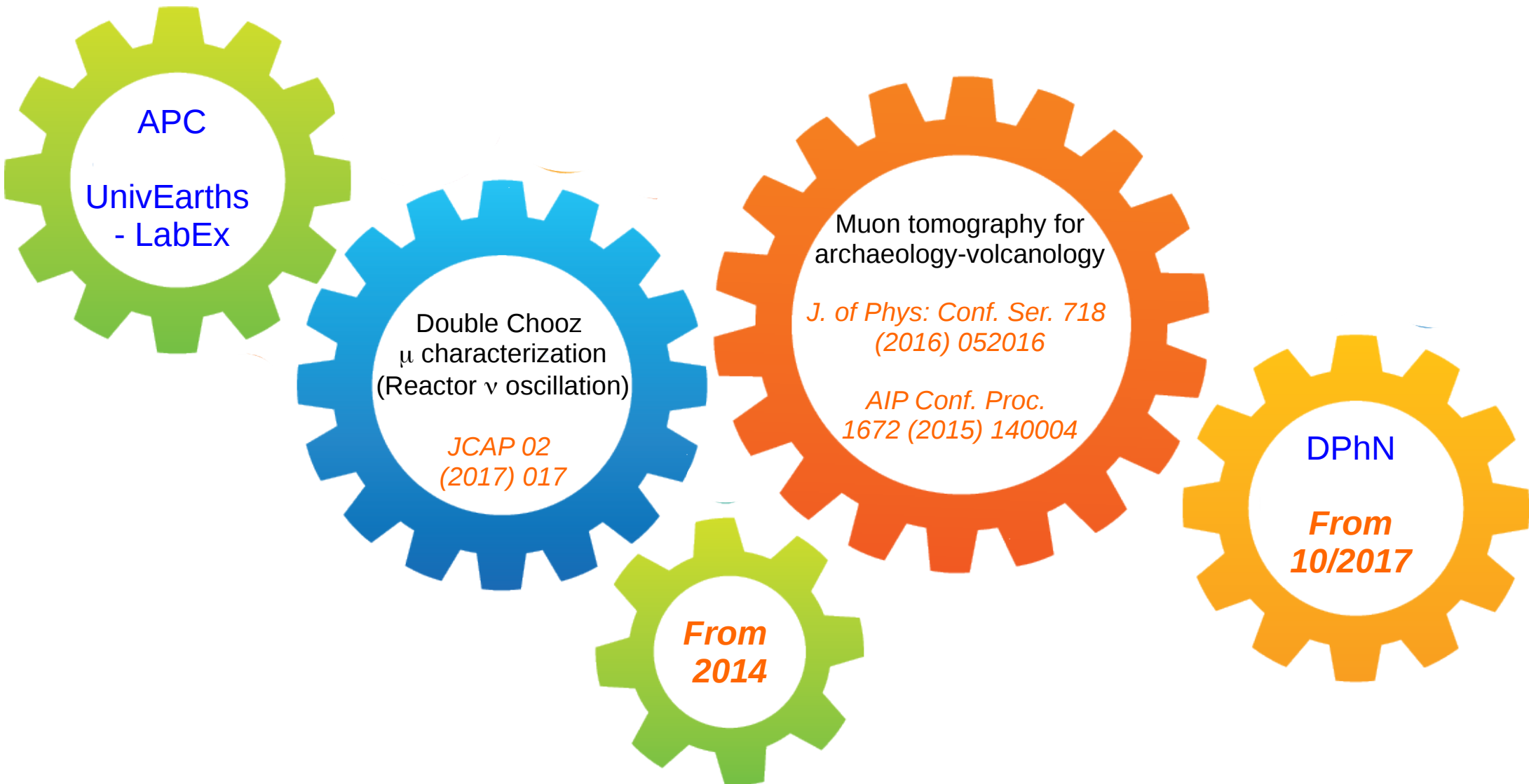
Héctor Gómez

IRFU / DPhN / LSN

hector.gomez@cea.fr





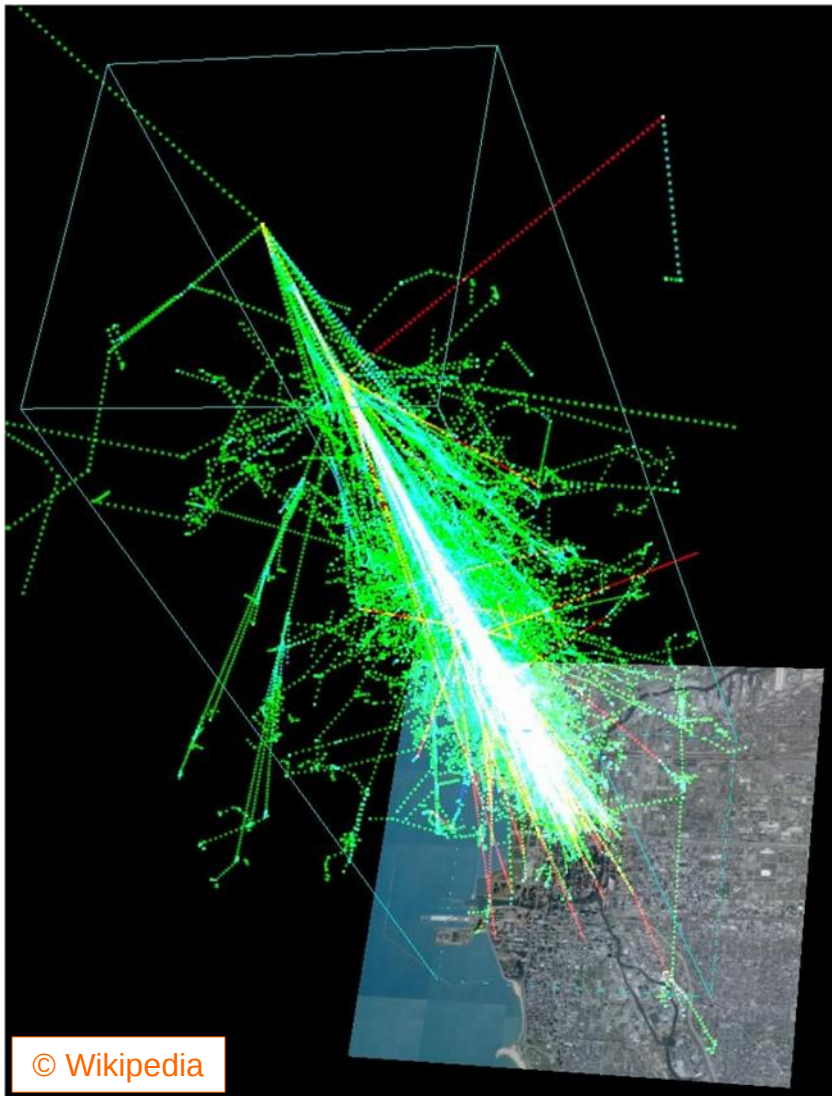


- Atmospheric muons
 - Main features
 - Background on Particle Physics: How to deal with them?

- Atmospheric muons and Reactor Neutrino experiments
 - The *Double Chooz* case
 - Muon characterization
 - Experimental data and Monte Carlo simulations → A “rough” muon tomography
 - Annual modulation: Effective temperature coefficient

- Taking advantage of muons
 - The muon tomography
 - The importance of simulations
 - Present and future applications

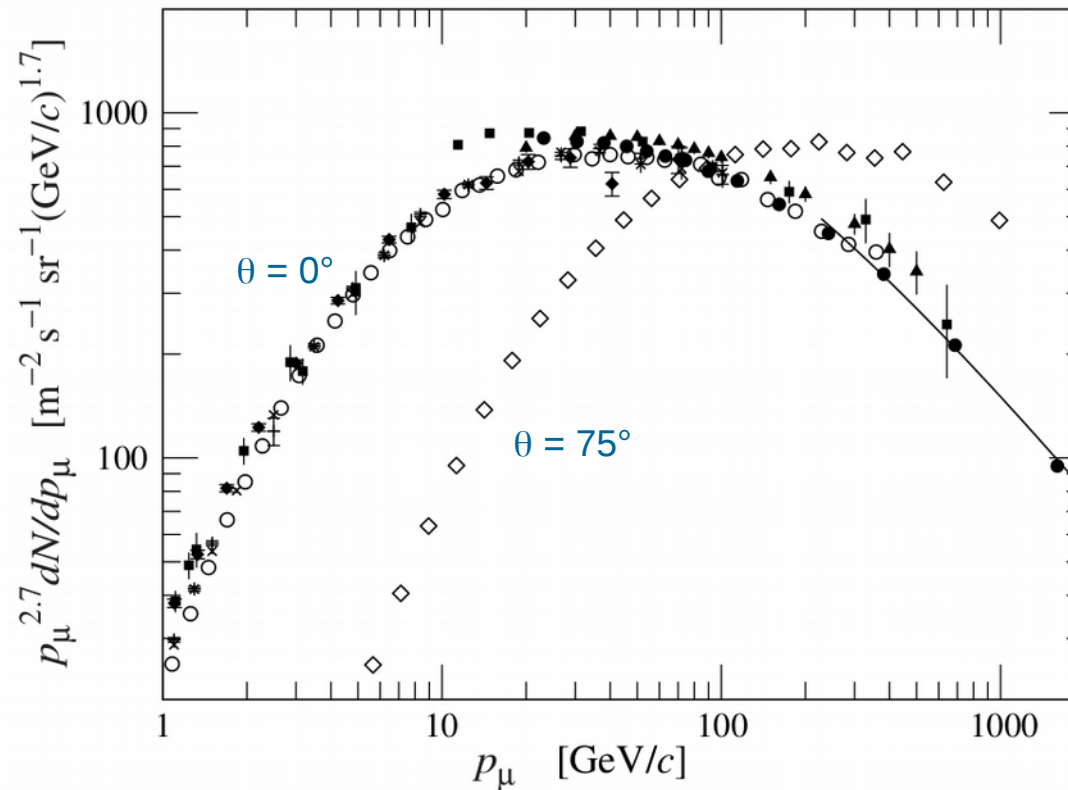
- Summary and conclusions



© Wikipedia

Simulation of the air-shower produced by a 1 TeV proton interacting in the atmosphere @ 20 km

- Muons produced by the interaction of cosmic-rays with nuclei of the Atmosphere
 - Also referred as cosmic-ray muons
 - Main component of the air-shower (together with the associated ν_μ , e^\pm and π^\pm).
 - Most of them produced high in the atmosphere
 - @ Earth's surface
 - E and angular distribution (θ) at surface is driven by:
 - Production spectrum
 - Energy loss along the path in the atmosphere
 - Muon decay
 - Mean energy ~ 4 GeV
 - Steepens along energy ($E_\mu > 1$ GeV)



Spectrum of muons for $\theta = 0^\circ$ and 75° obtained from different measurements (markers) and from the Gaisser parametrization (line)
 PDG. *Chin. Phys. C*, 40, 100001 (2016)

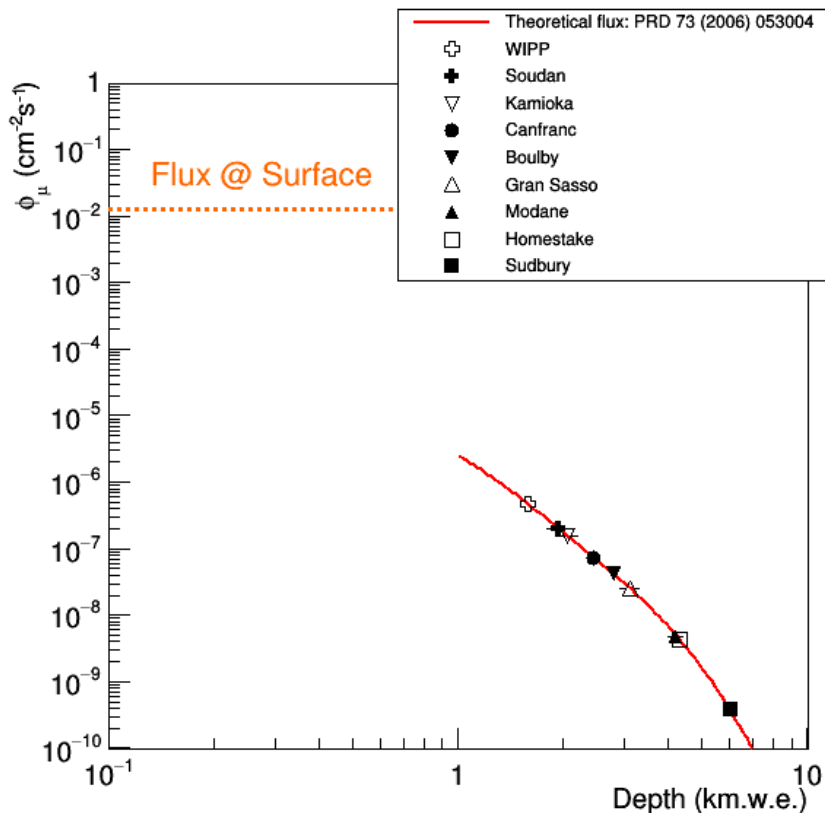
Muon flux @ surface (full θ range)

$$\Phi_\mu \sim 1.3 \cdot 10^{-2} \text{ cm}^{-2} \text{ s}^{-1}$$

- Atmospheric muons themselves and other muon-induced particles represent one of the most important background for Particle Physics experiments
- Ways to reduce / deal with this background:

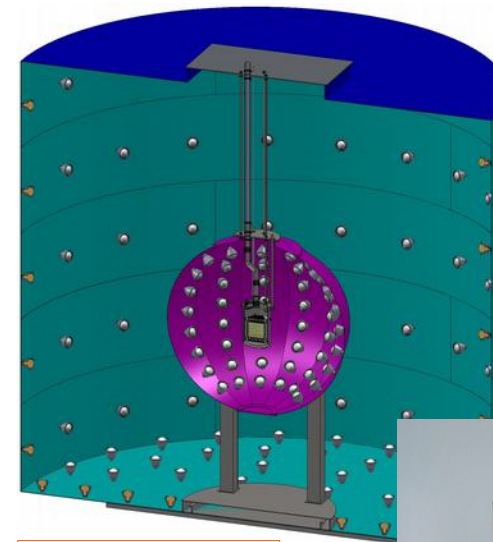
Passive methods

Going underground (Shielding): Mines, mountains...



Active methods

Dedicated detectors, tagging + analysis...



Dark Side @ Gran Sasso

Anais @ Canfranc

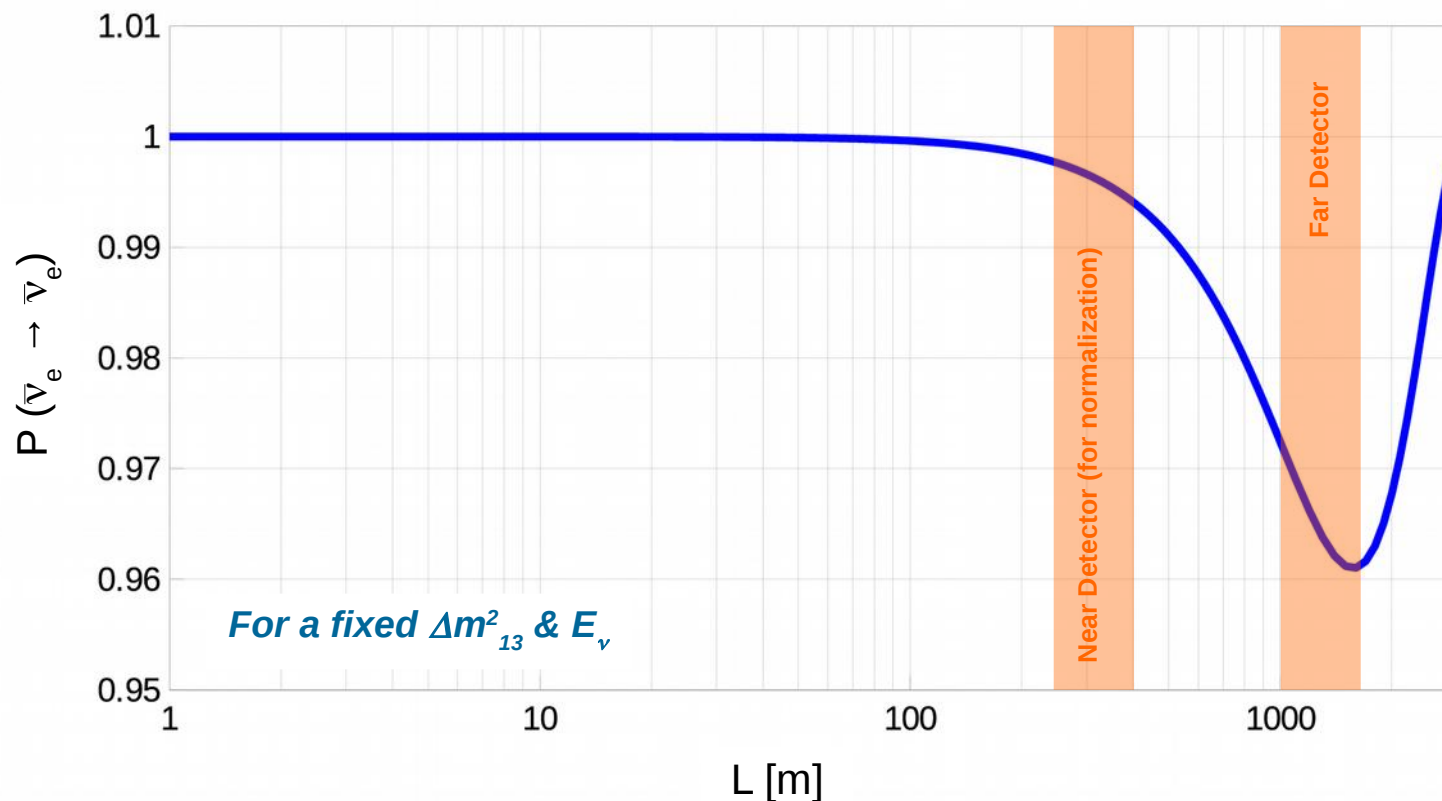


- **Short baseline experiments *in a nutshell*:**

- Determination of θ_{13} measuring the **deficit of detected anti-neutrinos** coming from the nuclear reactor

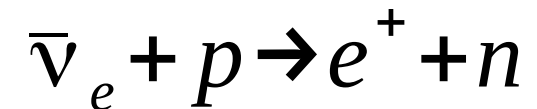
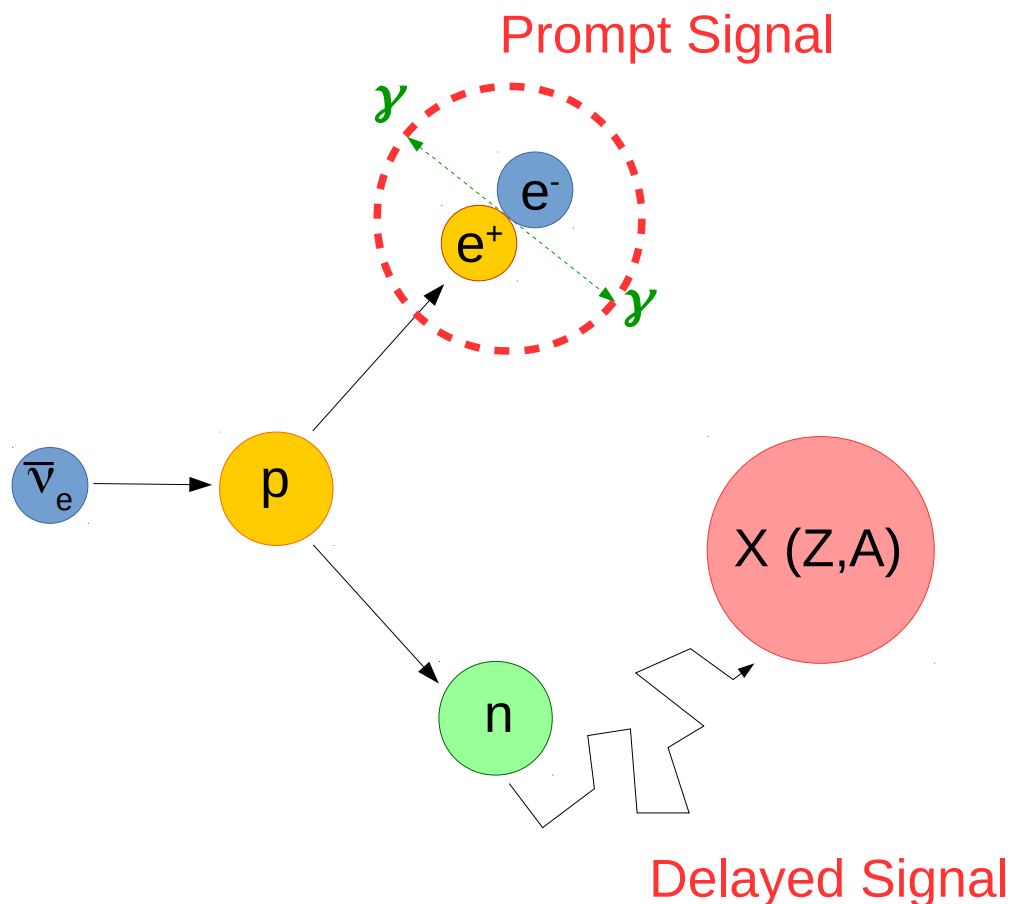
$$P(\bar{\nu}_e \rightarrow \bar{\nu}_e) = 1 - \sin^2(2\theta_{13}) \sin^2\left(\frac{\Delta m_{13}^2 L}{4 E_\nu}\right) + o(10^{-3})$$

$\left. \begin{array}{l} L \text{ [m]} / E \text{ [MeV]} \leq 1 \\ \text{No matter effects} \end{array} \right\}$



- **Short baseline experiments *in a nutshell*:**

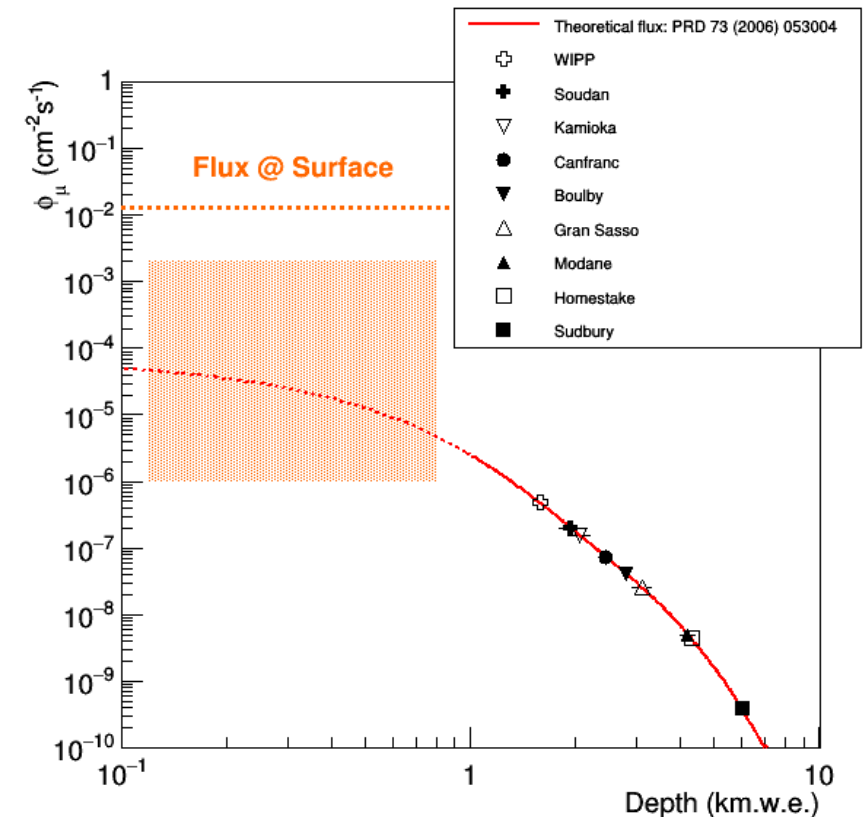
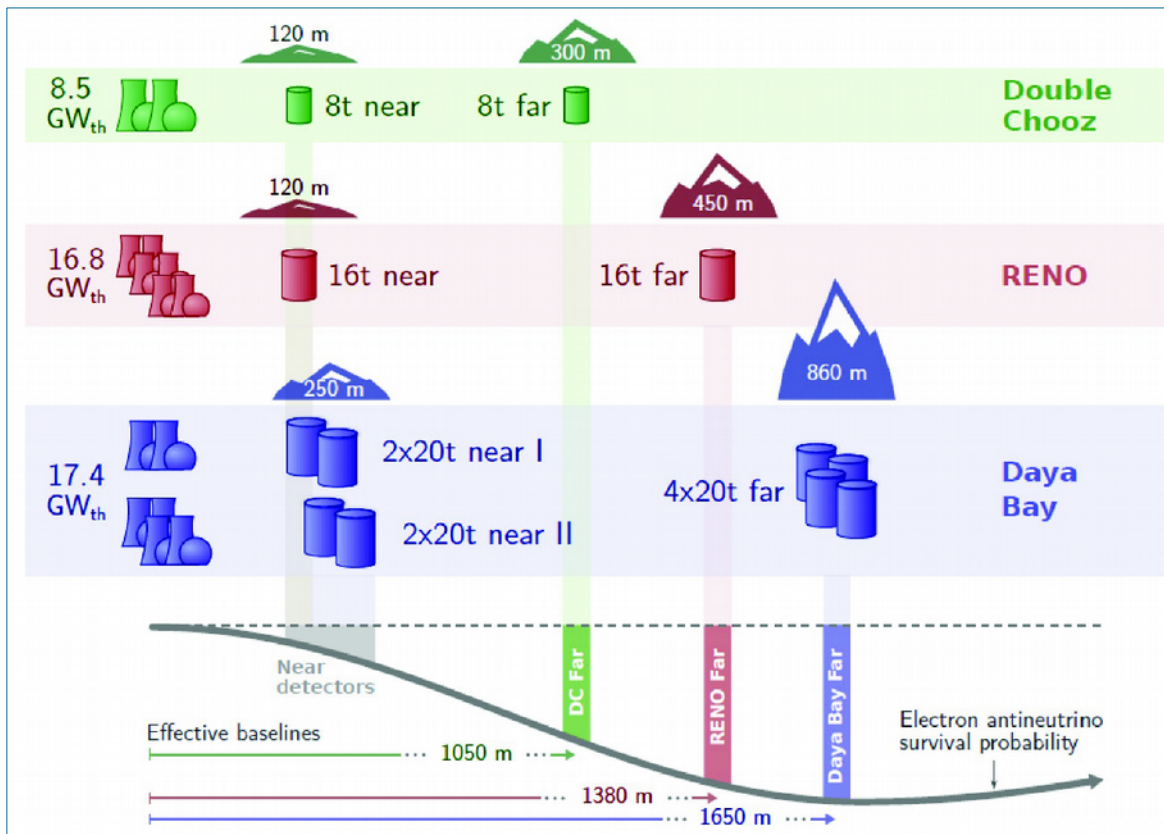
- Determination of θ_{13} measuring the **deficit of detected anti-neutrinos** coming from the nuclear reactor
- Anti-neutrinos detection ($E_{\bar{\nu}}$ < 10 MeV) via **Inverse Beta Decay (IBD)**

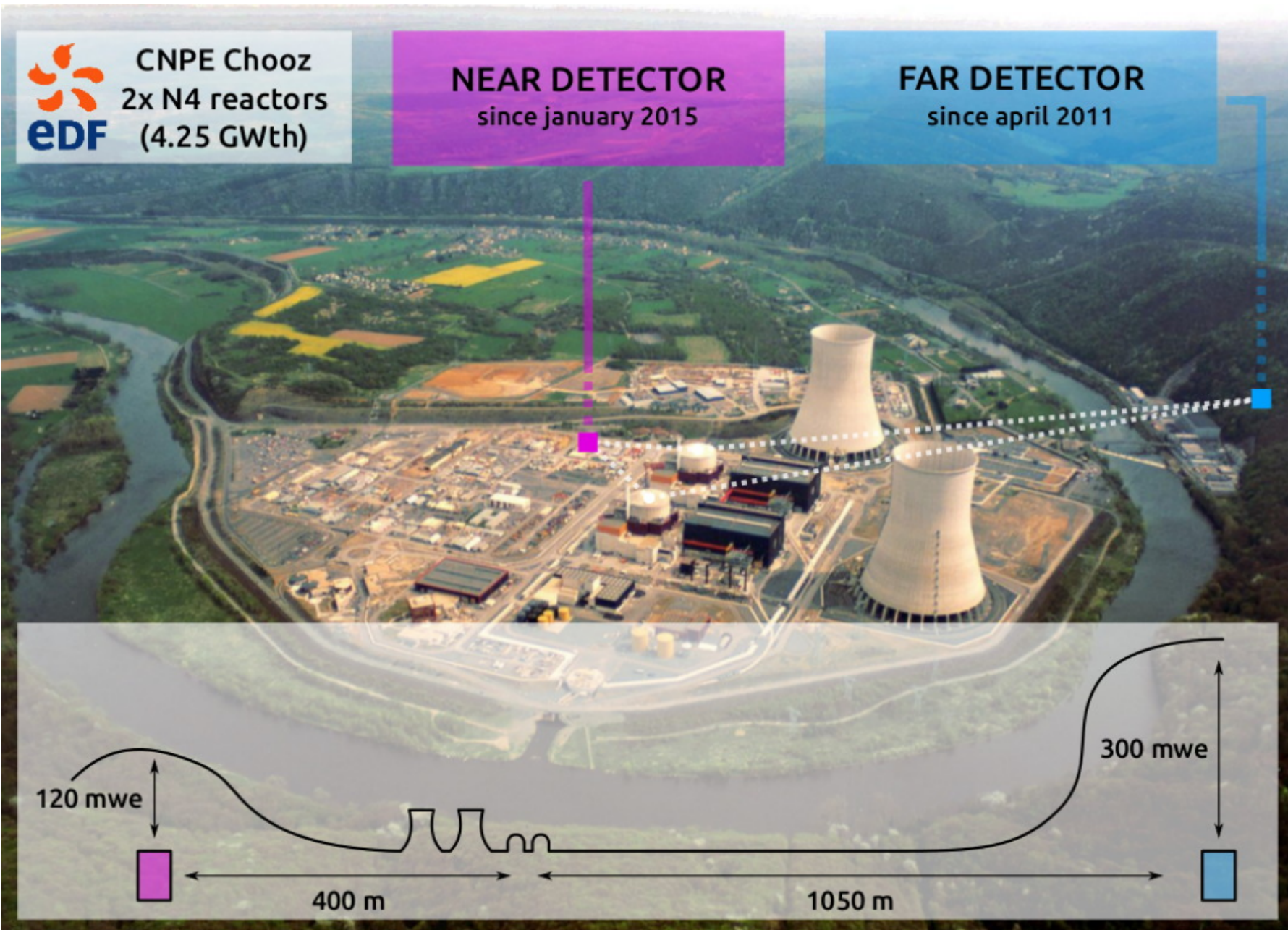


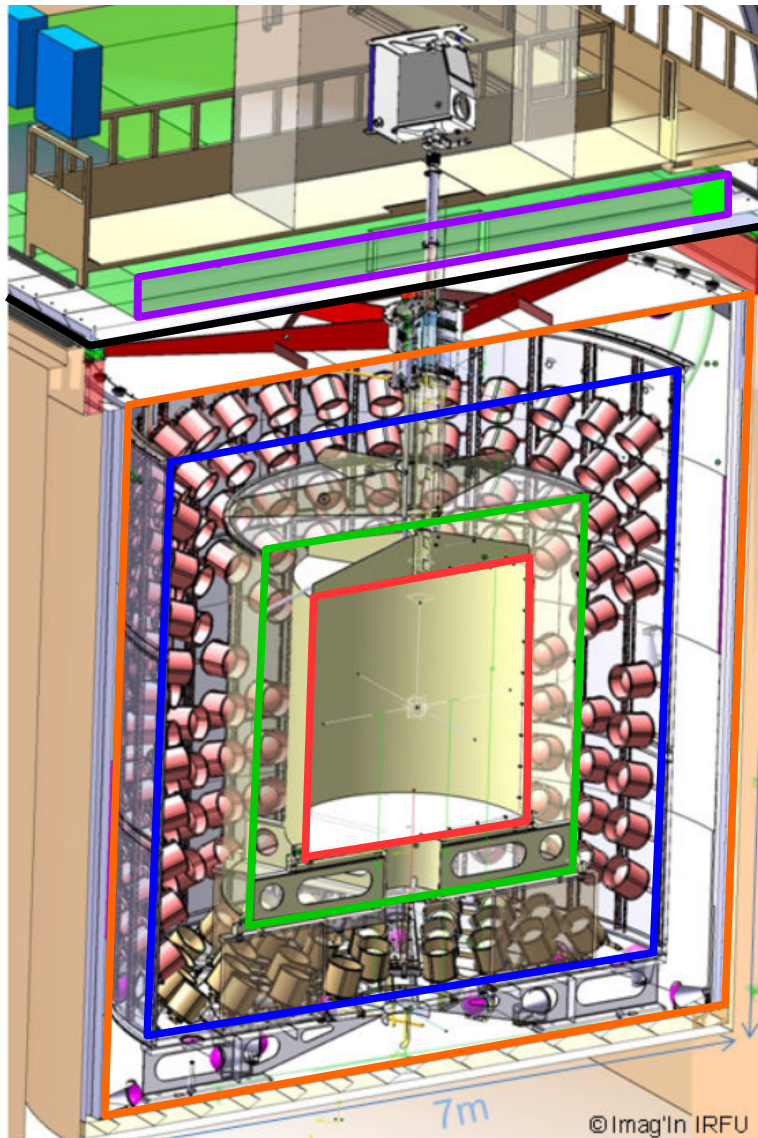
- Expected signal: Delayed coincidence
 - **Prompt Signal:** positron ionisation and annihilation
 - $E(e^+) \sim E(\bar{\nu}_e) - 0.8 \text{ MeV}$
 - Localized energy deposit
 - **Delayed signal:** nuclear neutron capture
 - Features depending on the nucleus
 - Energy released, delay time

- **Short baseline experiments *in a nutshell*:**

- Determination of θ_{13} measuring the **deficit of detected anti-neutrinos** coming from the nuclear reactor
- Anti-neutrinos detection ($E_\nu < 10$ MeV) via **Inverse Beta Decay (IBD)**
- Three main experiments in the world: Daya Bay, **Double Chooz** and Reno







LAYOUT:

ν - Target

10.3 m³ liquid scintillator, doped with 1 g/l of Gd in an 8 mm thick acrylic vessel.

Gamma Catcher

22.6 m³ liquid scintillator in a 12 mm thick acrylic vessel

Buffer

110 m³ of mineral oil (non-scintillating) in a 3 mm thick Stainless Steel vessel. It holds **390 PMTs (10 inches)** working as readout

Inner Veto

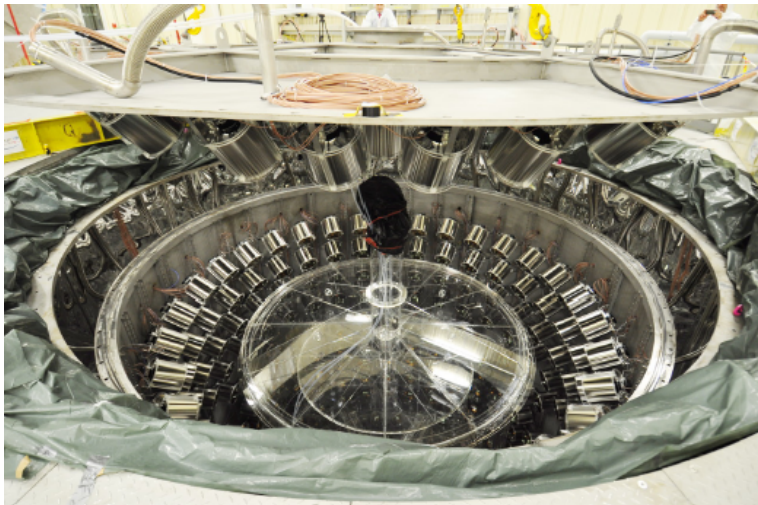
90 m³ liquid scintillator in a 10 mm thick Stainless Steel vessel equipped with 78 PMTs (8 inches)

Upper Shielding

15 cm thick steel plates

Outer Veto

Plastic scintillator panels



LAYOUT:

Inner detector (ID)

ν - Target

10.3 m³ liquid scintillator, doped with 1 g/l of Gd in an 8 mm thick acrylic vessel.

Gamma Catcher

22.6 m³ liquid scintillator in a 12 mm thick acrylic vessel

Buffer

110 m³ of mineral oil (non-scintillating) in a 3 mm thick Stainless Steel vessel. It holds **390 PMTs (10 inches)** working as readout

Inner Veto

90 m³ liquid scintillator in a 10 mm thick Stainless Steel vessel equipped with 78 PMTs (8 inches)

Upper Shielding

15 cm thick steel plates

Outer Veto

Plastic scintillator panels

Signal

- **Two** antineutrino identification **channels** (both based on IBD)



- Neutron capture by **Gd** nuclei (**baseline**)

- Delayed signal: **$E \sim 8 \text{ MeV}; \Delta t \sim 30 \mu\text{s}$**

- **✓** Well above natural background

- **✗** Limited fiducial volume (ν - target)

- Neutron capture by **H** nuclei

- Delayed signal: **$E \sim 2.2 \text{ MeV}; \Delta t \sim 200 \mu\text{s}$**

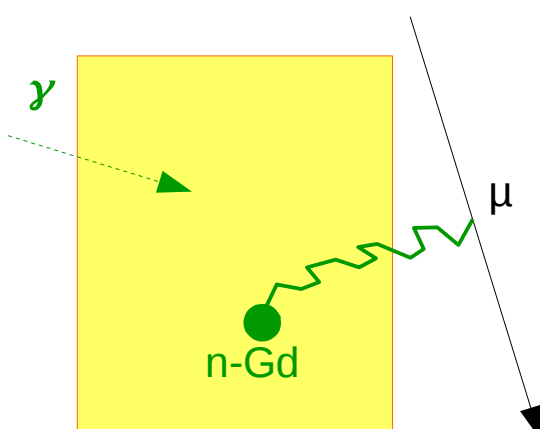
- **✓** Increase of the sensitive volume (ν - target + gamma catcher)

- **✗** More background expected

- **✗** Natural background

- **✗** Accidentals (bigger delay) \rightarrow Additional background rejection tools required

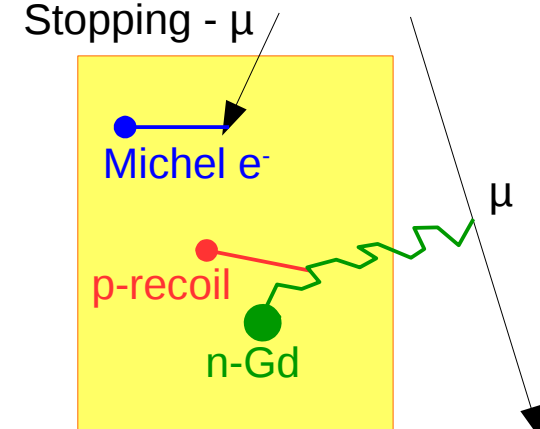
Backgrounds



Accidental Coincidences

Natural Radioactivity

e.g. γ + spallation n

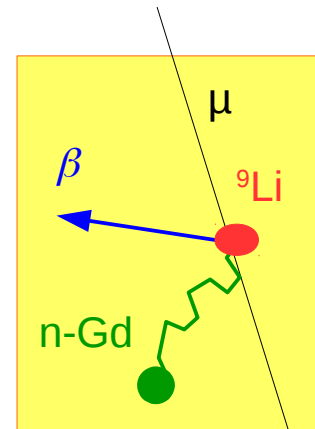


Stopping - μ

Correlated Events

Fast neutrons & Stopping - μ

$$n + p \rightarrow p + n$$

$$\mu \rightarrow e + \nu + \bar{\nu}$$


Cosmogenic Isotopes

β - n emitters (${}^9\text{Li}$ & ${}^8\text{He}$)

$${}^9\text{Li} \rightarrow \alpha + \alpha + e + \nu + n$$

Backgrounds

Accidental Coincidences

Natural Radioactivity

e.g. γ + spallation n

Stopping - μ

Correlated Events

Fast neutrons & Stopping - μ

$n + p \rightarrow p + n$

$\mu \rightarrow e + \nu + \nu$

Cosmogenic Isotopes

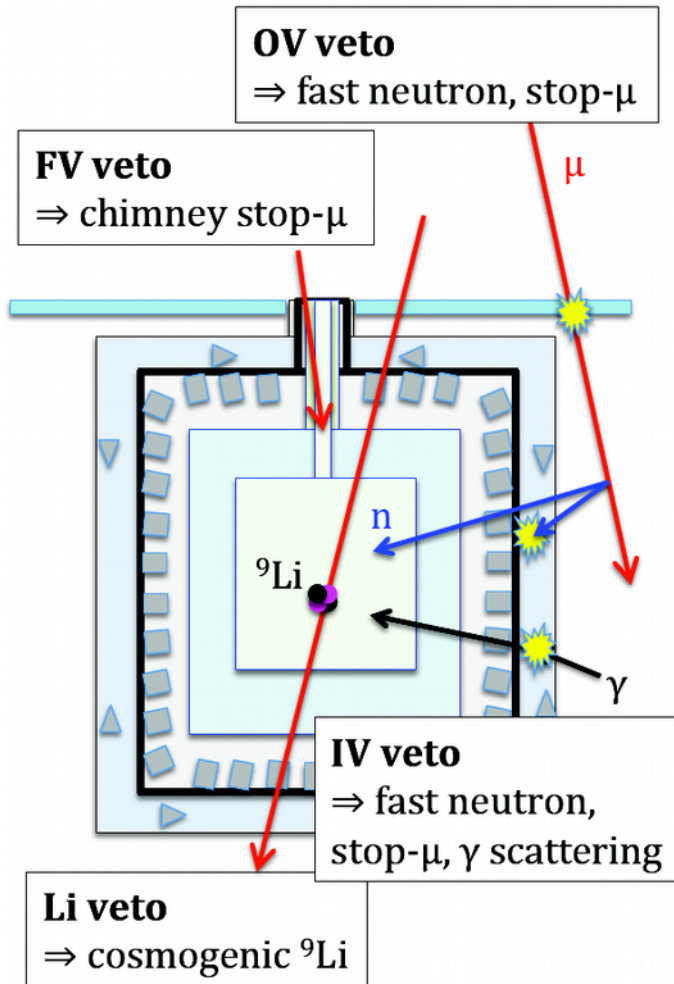
β - n emitters (${}^9\text{Li}$ & ${}^8\text{He}$)

${}^9\text{Li} \rightarrow \alpha + \alpha + e + \nu + n$

- Prompt signal
- Delayed signal

Development of dedicated background rejection techniques...

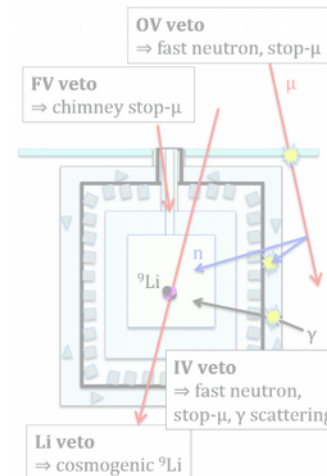
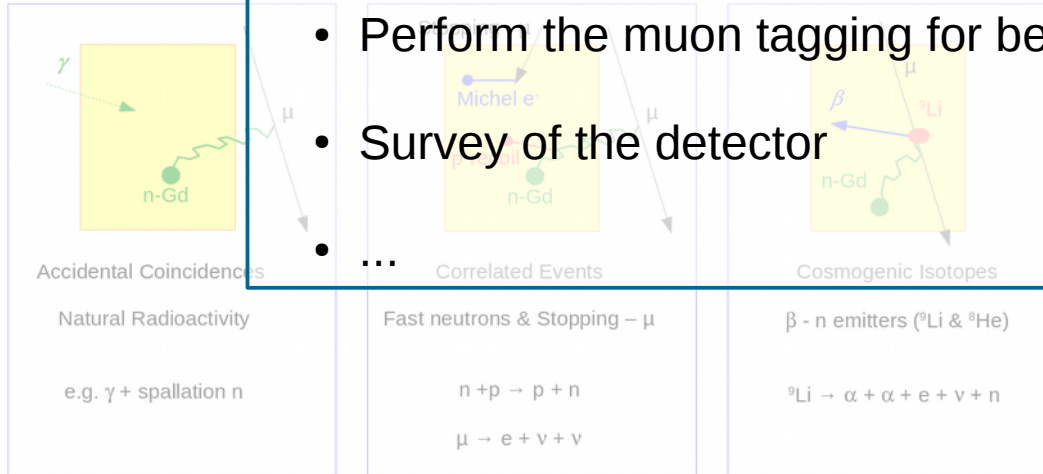
Backgrounds



Cut	Information used	Target of cut
μ veto	1 ms veto after μ	μ , cosmogenics
Multiplicity	Uniqueness condition	Multiple n's
FV veto	Vertex likelihood	Chimney stopping μ
IV veto	IV activity	Fast n, stopping μ , γ scattering
OV veto	OV activity	Fast n, stopping μ
Li veto	Li Likelihood	Cosmogenics
LN cut	PMT hit pattern and time	Light emission from PMT
ANN	$E_{\text{delayed}}, \Delta T, \Delta R$	Accidentals
MPS veto	Pulses start time	Fast n
CPS veto	Chimney likelihood	Stopping μ
Q ratio	Max. Q / Tot. Q	ND Buffer stopping μ

Only applied in n – H analysis
Only applied in the multi-detector analysis

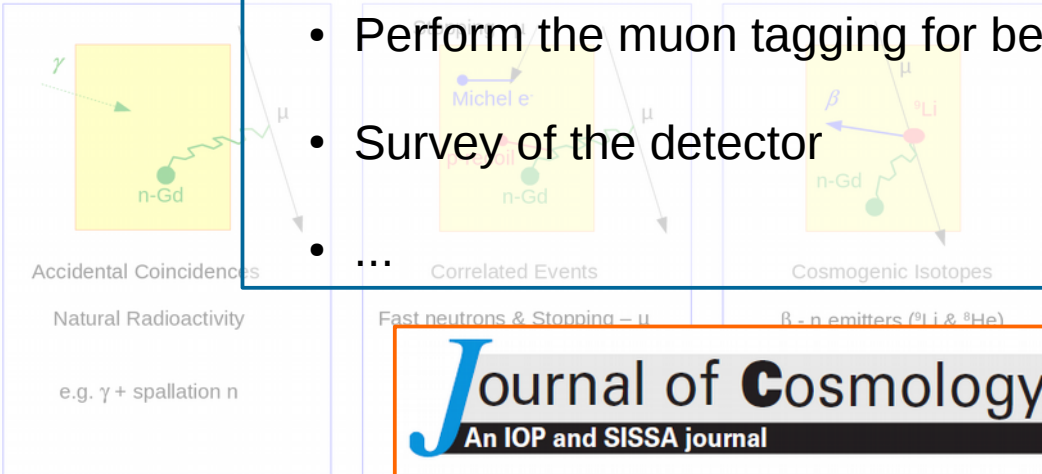
- Complete muon characterization is useful to:
 - Better understand Double Chooz background features
 - Perform the muon tagging for better identification of μ – induced events
 - Survey of the detector



Cut	Information used	Target of cut
μ veto	1 ms veto after μ	μ , cosmogenics
Multiplicity	Uniqueness condition	Multiple n 's
FV veto	Vertex likelihood	Chimney stopping μ
IV veto	IV activity	Fast n , stopping μ , γ scattering
OV veto	OV activity	Fast n , stopping μ
Li veto	Li Likelihood	Cosmogenics
LN cut	PMT hit pattern and time	Light emission from PMT
ANN	E_{delayed} , ΔT , ΔR	Accidentals
MPS veto	Pulses start time	Fast n
CPS veto	Chimney likelihood	Stopping μ
Q ratio	Max. Q / Tot. Q	ND Buffer stopping μ

Only applied in $n - H$ analysis
Only applied in the multi-detector analysis

- Complete muon characterization is useful to:
 - Better understand Double Chooz background features
 - Perform the muon tagging for better identification of μ – induced events
 - Survey of the detector



Journal of **C**osmology and **A**stroparticle **P**hysics
An IOP and SISSA journal

Cosmic-muon characterization and annual modulation measurement with Double Chooz detectors

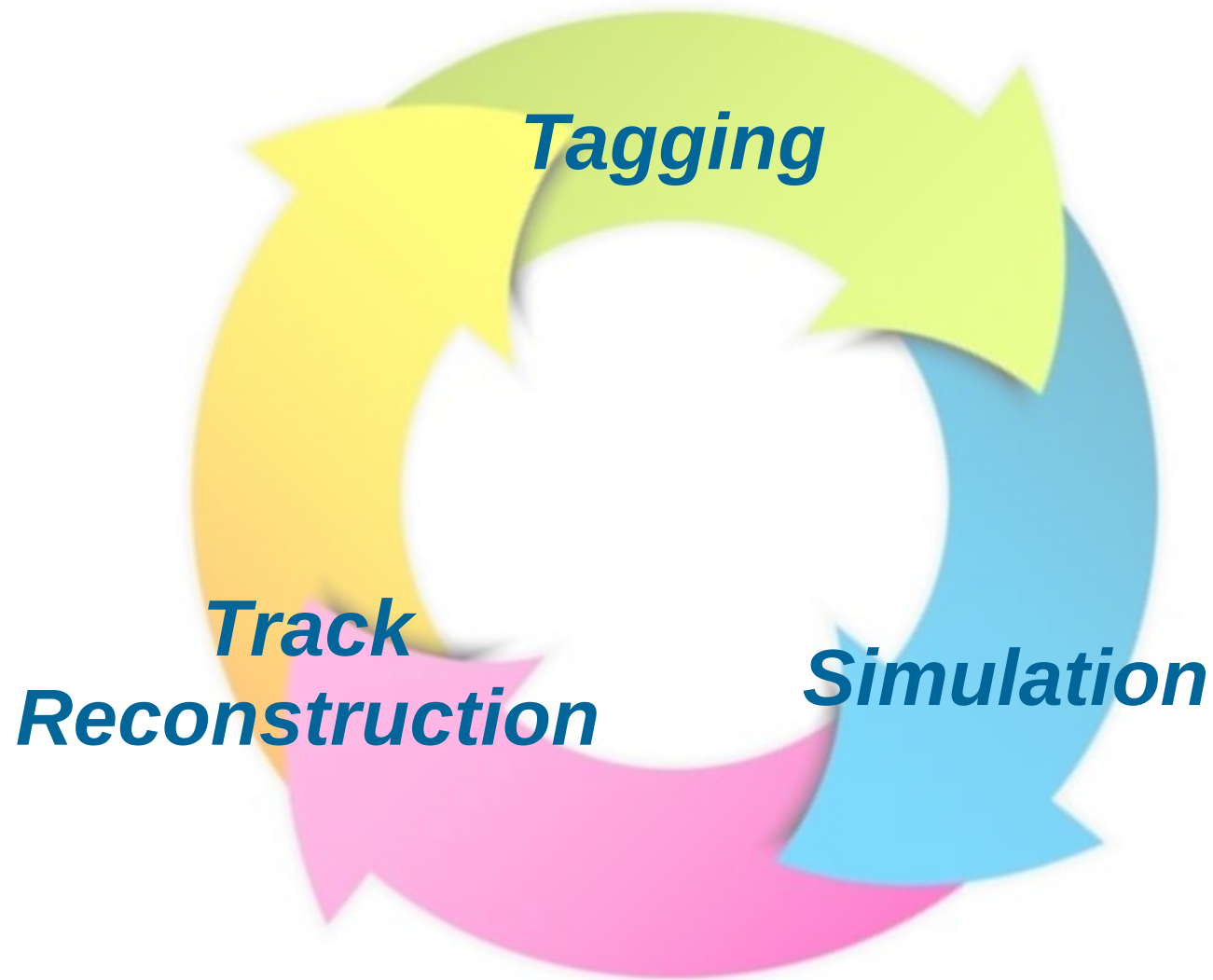


The Double Chooz collaboration

JCAP 02 (2017) 017

Condition used	Target of cut
Time after μ	μ , cosmogenics
Neutron condition	Multiple n's
Stopping likelihood	Chimney stopping μ
Activity	Fast n, stopping μ , γ scattering
Activity	Fast n, stopping μ
Stopping likelihood	Cosmogenics
Light pattern time	Light emission from PMT
$\Delta T, \Delta R$	Accidentals
Start time	Fast n
Stopping likelihood	Stopping μ
$Q / Tot. Q$	ND Buffer stopping μ

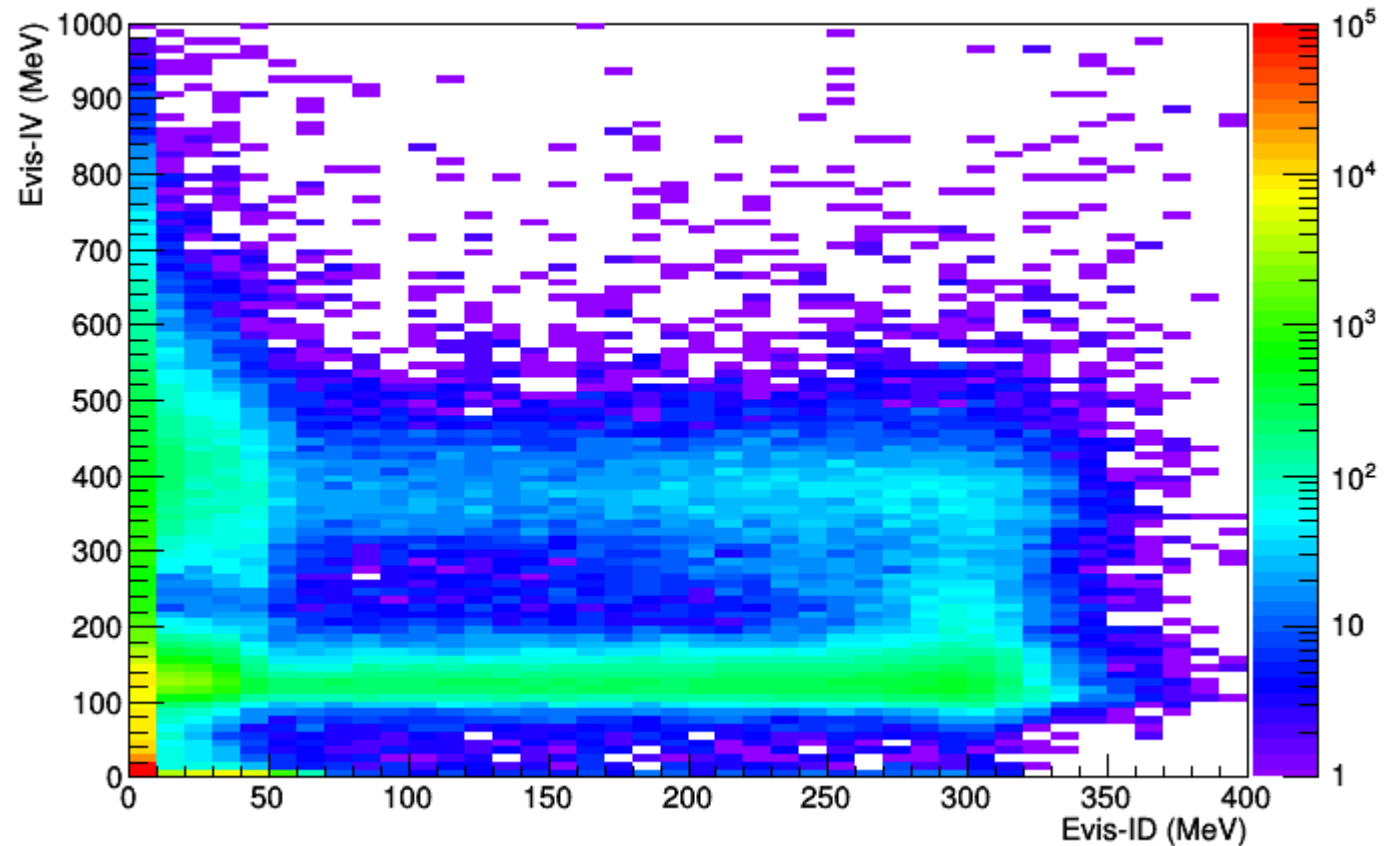
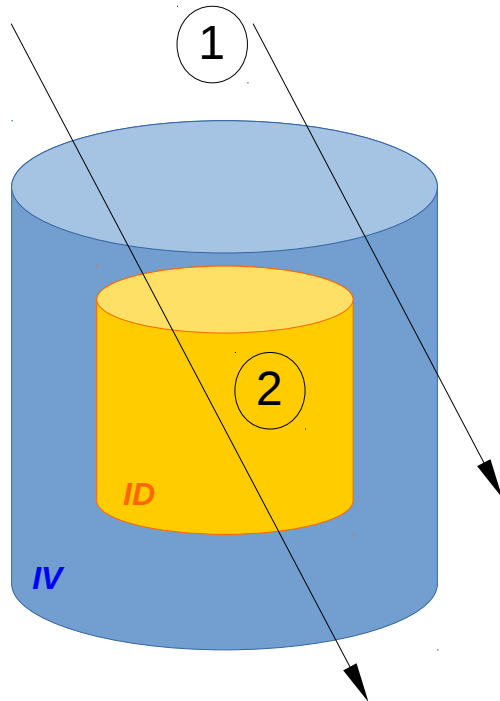
Only applied in n – H analysis
Only applied in the multi-detector analysis



Tagging

- Muons deposit large amounts of energy ($\sim 2 \text{ MeV cm}^2 / \text{g}$ for liquid scintillators) if compared with other particles when they traverse the sensitive volumes of Double Chooz detectors i.e. Inner Detector (ID) and Inner Veto (IV)

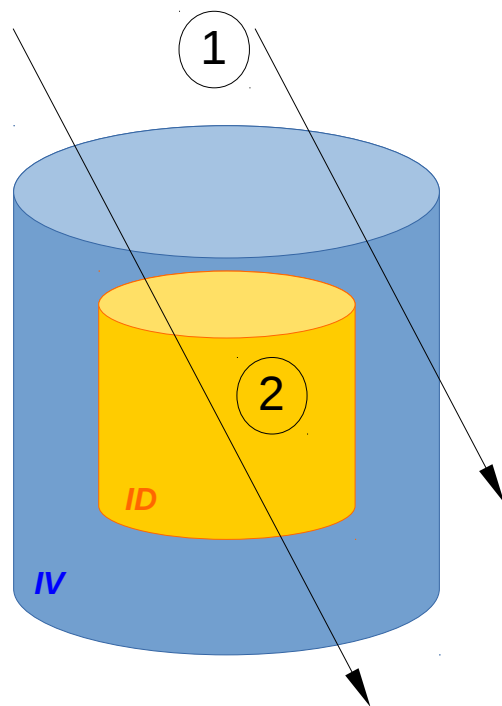
$$\frac{-dE}{dX} = 4 \pi N_0 r_e^2 m_e c^2 Z_a^2 \frac{Z}{A} \frac{1}{\beta^2} \left[\frac{1}{2} \ln \left(\frac{2 m_e c^2 \beta^2 \gamma^2 T_{max}}{I^2} \right) - \beta^2 - \frac{\delta(\beta \gamma)}{2} - \frac{C}{Z} \right]$$



Tagging

- Muons deposit large amounts of energy ($\sim 2 \text{ MeV cm}^2 / \text{g}$ for liquid scintillators) if compared with other particles when they traverse the sensitive volumes of Double Chooz detectors i.e. Inner Detector (ID) and Inner Veto (IV)

$$\frac{-dE}{dX} = 4 \pi N_0 r_e^2 m_e c^2 Z_a^2 \frac{Z}{A} \frac{1}{\beta^2} \left[\frac{1}{2} \ln \left(\frac{2 m_e c^2 \beta^2 \gamma^2 T_{max}}{I^2} \right) - \beta^2 - \frac{\delta(\beta \gamma)}{2} - \frac{C}{Z} \right]$$



Standard selection (deposited energy in scintillating volumes)

1: $E_{vis-IV} > 25 \text{ MeV}$

2: $E_{vis-ID} > 30 \text{ MeV}$ and $E_{vis-IV} > 5 \text{ MeV}$

Mean Muon Rate*:

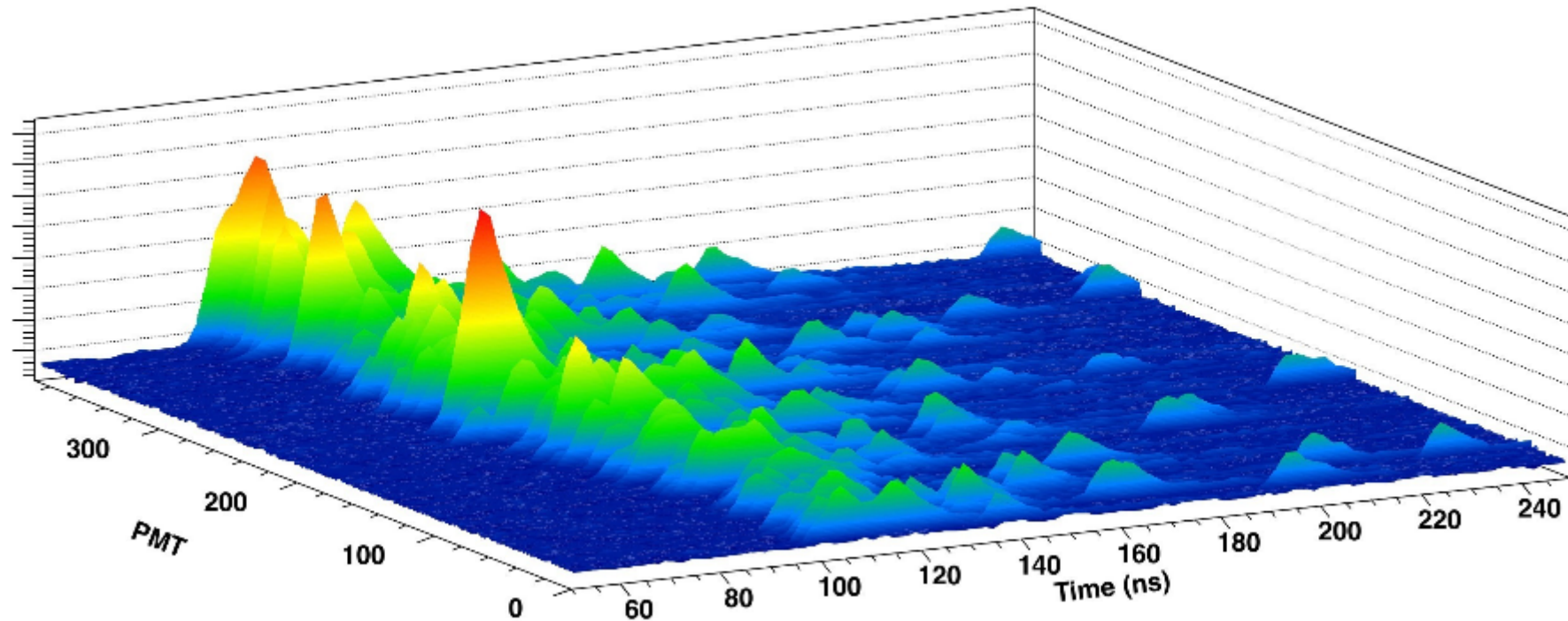
Near detector: $\langle R_\mu \rangle = 242.75 \pm 4.81 \text{ Hz} \rightarrow \sim 75 \%$ of the total rate

Far detector: $\langle R_\mu \rangle = 46.16 \pm 1.04 \text{ Hz} \rightarrow \sim [8 - 20] \%$ of the total rate

*Mean rate for all the analysed data: ~ 151 and ~ 673 days for the near and far detectors respectively

Track Reconstruction

Nucl. Instrum. Meth. A 764 (2014) 330



Ingredients:

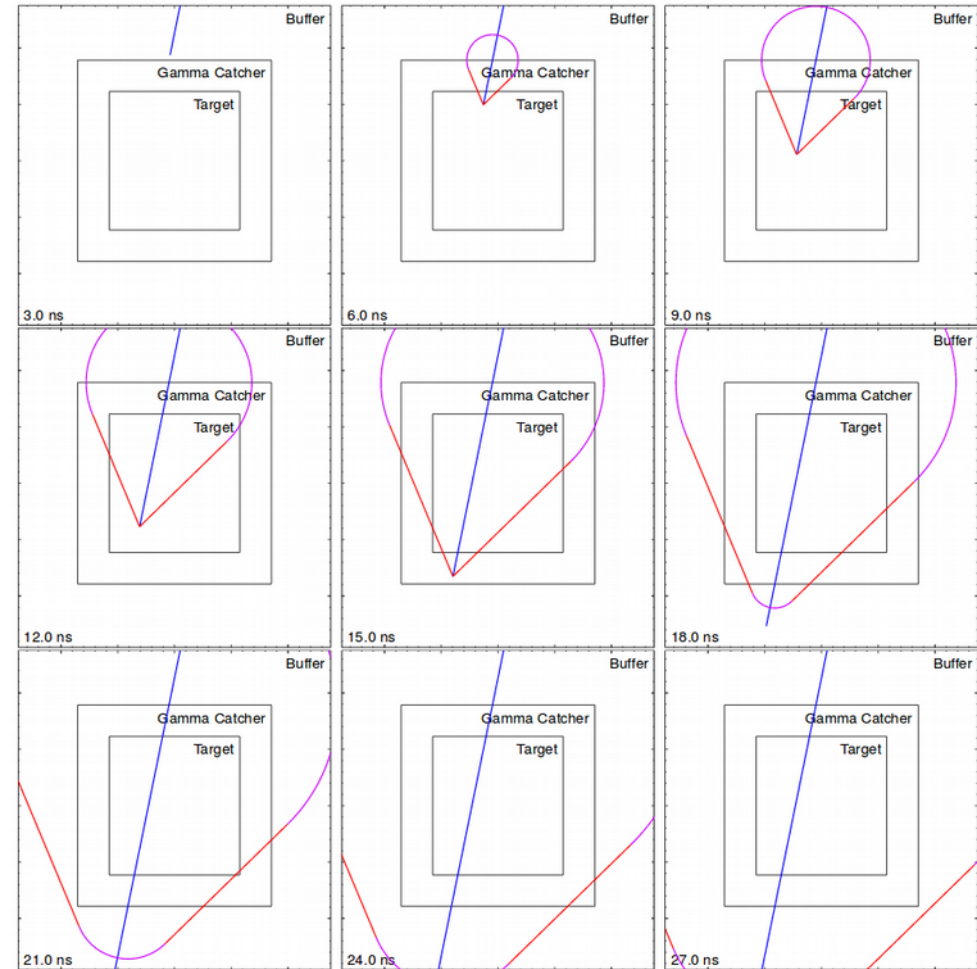
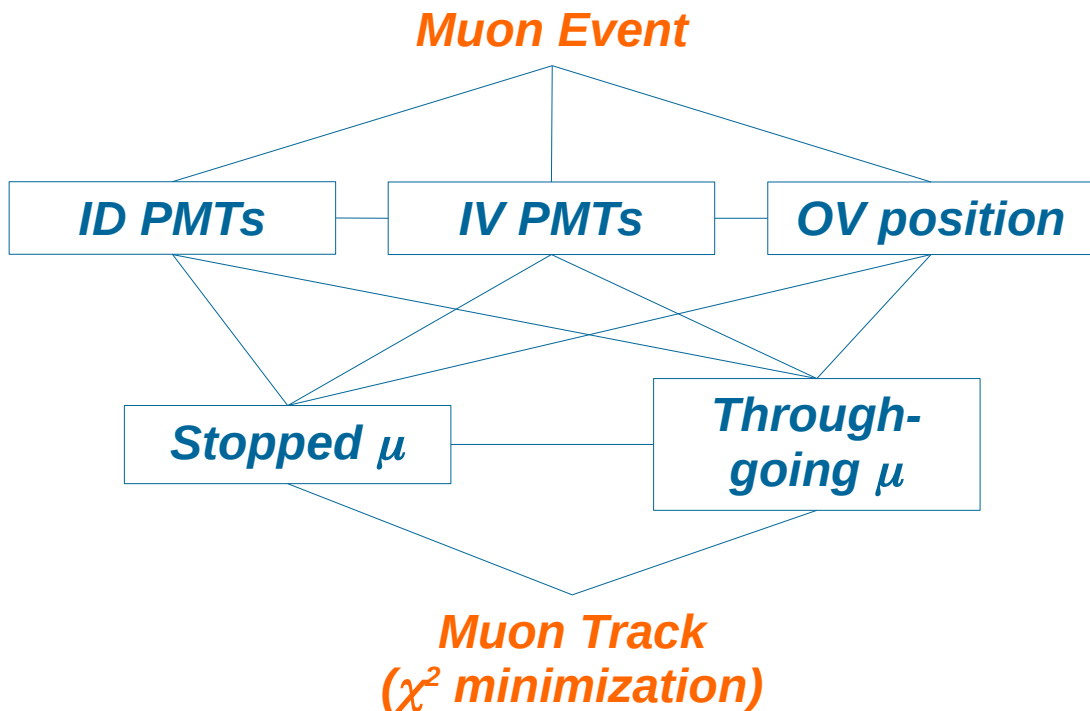
- Pulse reconstruction for all the fired (ID and IV) PMTs → Charge and Time information
- Spatial information of the Outer Veto

Track Reconstruction

Nucl. Instrum. Meth. A 764 (2014) 330

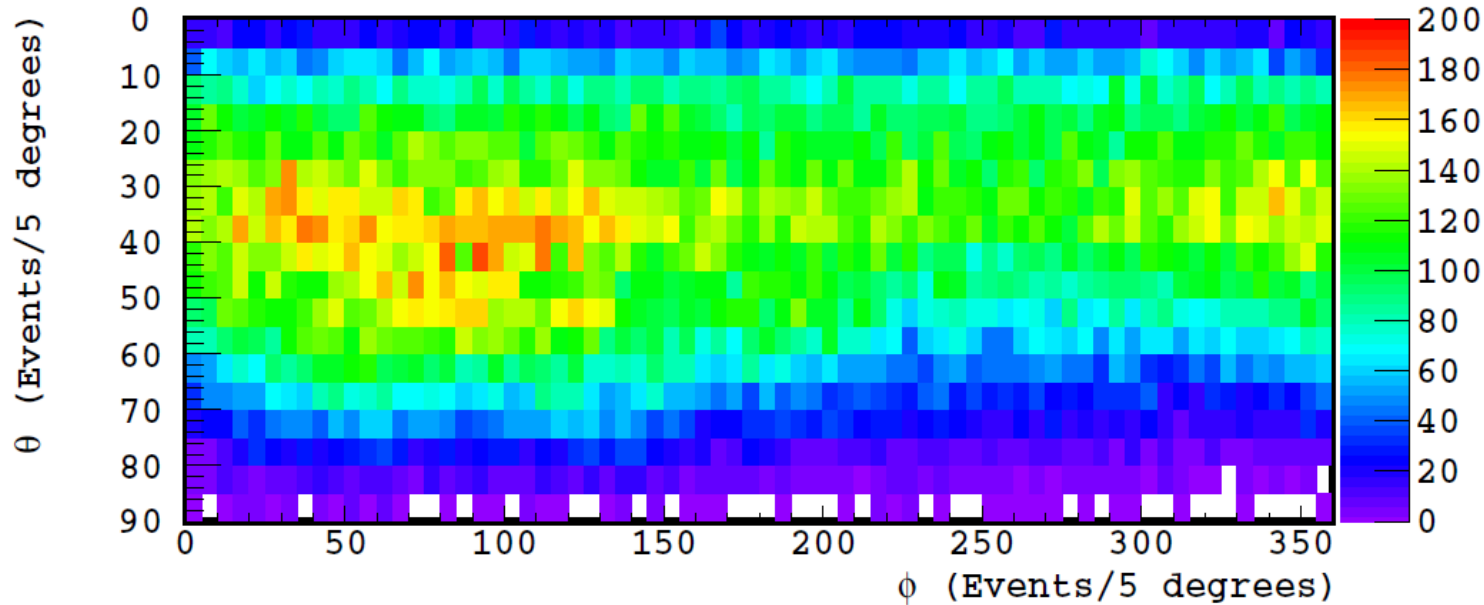
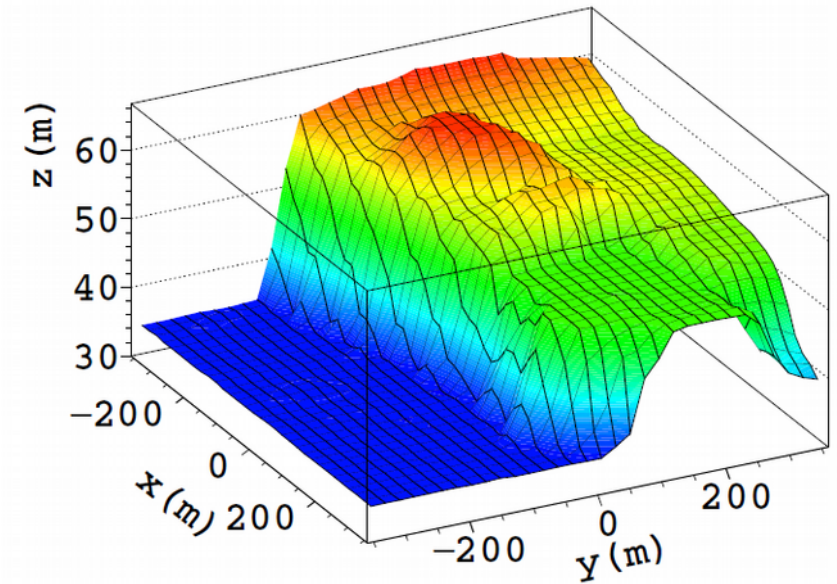
Fit process:

- Multiple fits with different combinations
- All assuming Cherenkov and scintillation light



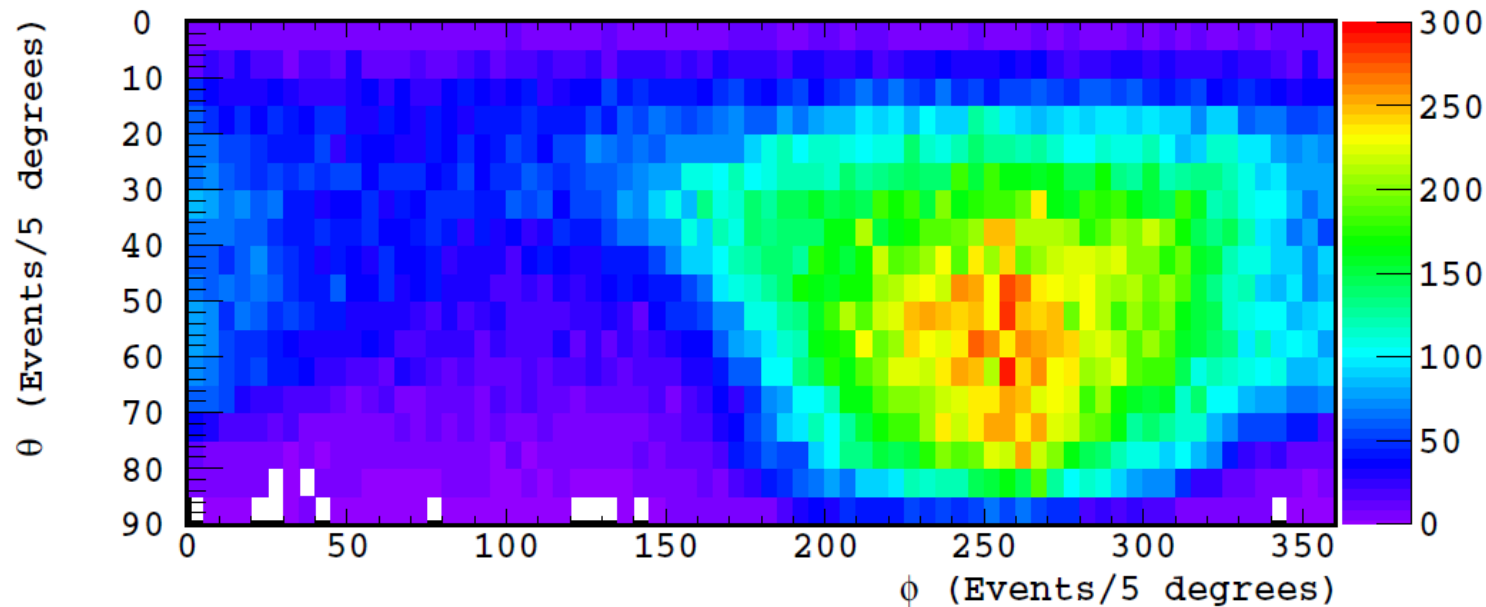
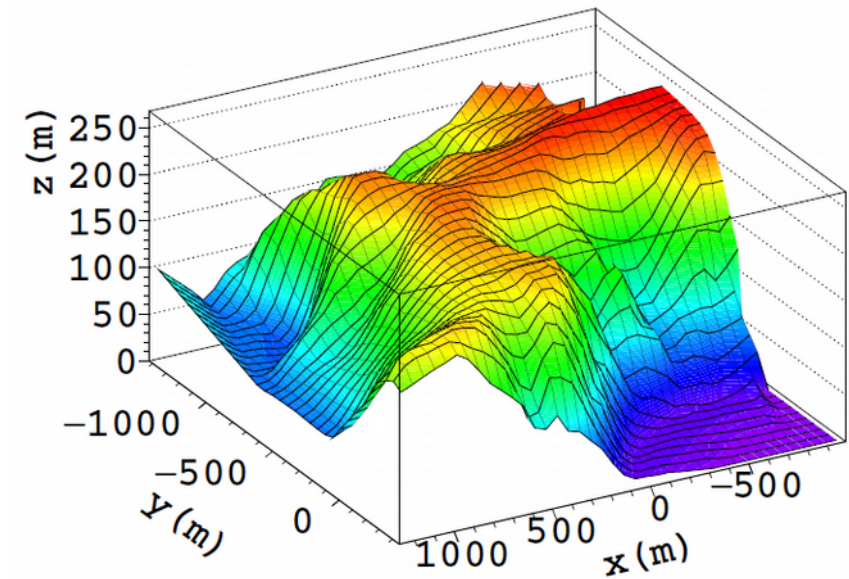
Tagging + Tracking → Angular distributions

- **Near detector:**
 - Digitized overburden profile from IGN
 - Homogeneous sampling mesh of 5x5 m



Tagging + Tracking \rightarrow Angular distributions

- **Far detector:**
 - 3DField digitization from a topographic study
 - Smaller mesh for less inhomogeneous regions

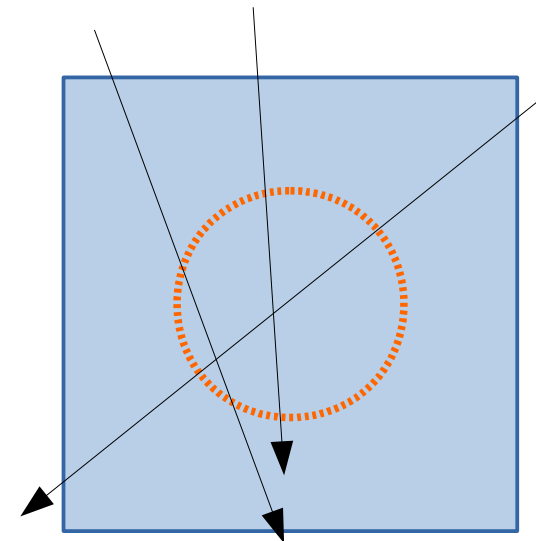


Tagging + Tracking → Muon flux

- Flux reconstructed via the so-called “*sphere method*” which uses the muon rate (tagging) and the track information (minimum track distance to detector centre)

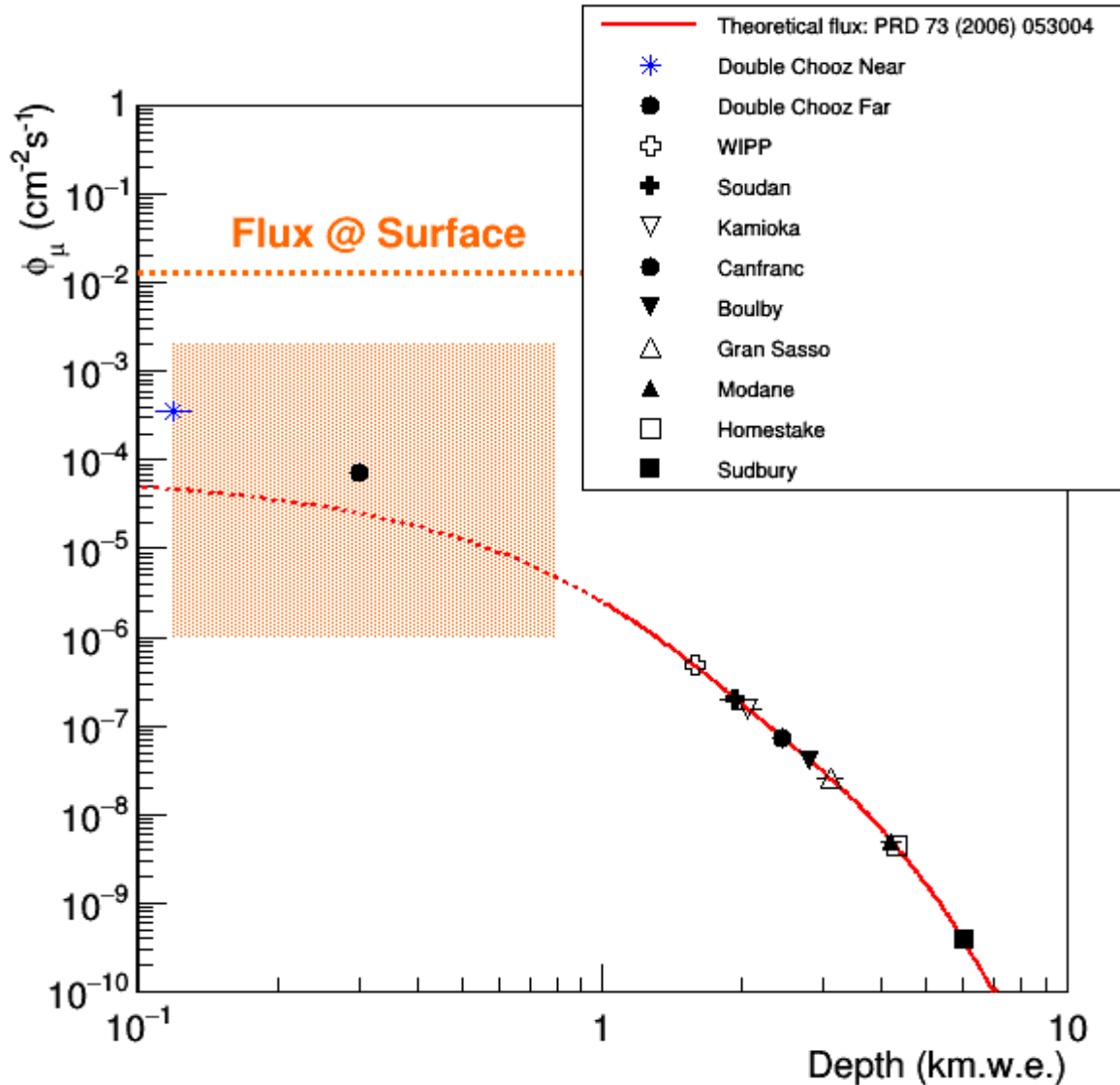
$$\phi_{\mu} = \frac{\langle R_{\mu} \rangle}{S_{eff}}$$

- For a cylindrical detector, S_{eff} is a function of θ and ϕ
→ More difficult to compute
- For a spherical detector, $S_{eff} = \pi R^2$ for all directions
→ Simpler and with lower uncertainties



- Selecting μ crossing at a radial distance smaller than $R \rightarrow S_{eff} = \pi R^2$
- This radial distance can be computed from the track reconstruction algorithm

Tagging + Tracking → Muon flux



Near Detector: $\phi_{\mu} = 3.64 \pm 0.04 \cdot 10^{-4} \text{ cm}^{-2} \text{ s}^{-1}$

Far Detector: $\phi_{\mu} = 7.00 \pm 0.05 \cdot 10^{-5} \text{ cm}^{-2} \text{ s}^{-1}$

~1% accuracy

Simulations

- Simulations have been performed using the **MUSIC** simulation package
Astroparticle Physics 7 (1997) 357 – 368
 - Routine to implement in your code to simulate the **transport of muons through materials**
 - ✓ Faster than other simulations packages (e.g. Geant 4) → Specially useful for long μ paths
 - ✓ Versatile: Not difficult to implement the digitized overburden profiles
 - ✗ Consider internal structures/anomalies → Concatenate simulations
 - ✗ Detector response to do “off-line”



Simulations

- Simulations have been performed using the **MUSIC** simulation package
Astroparticle Physics 7 (1997) 357 – 368
 - Routine to implement in your code to simulate the **transport of muons through materials**
 - ✓ Faster than other simulations packages (e.g. Geant 4) → Specially useful for long μ paths
 - ✓ Versatile: Not difficult to implement the digitized overburden profiles
 - ✗ Consider internal structures/anomalies → Concatenate simulations
 - ✗ Detector response to do “off-line”

Overburden Profile and Composition

Muon Distribution at Surface

$$N_{\mu}(E_{\mu}, \theta, \phi)$$

Simulations

- Due to the low overburden (120 and 300 m.w.e.) muons down to 20 and 40 GeV respectively are able to reach the detectors
 - ➔ It is for low energies where muon models present more differences
- Comparing simulations between them and w.r.t. experimental data would allow to validate these models

Extended Gaisser parametrization:

Phys. Rev. D 74 (2006) 053007

- ✓ Based on Gaisser analytical formula ($E_\mu > 100/\cos(\theta)$ GeV)
- Originally not valid for low energy; valid extension?

CRY generation:

http://nuclear.llnl.gov/simulation/doc_cry_v1.7/cry.pdf

- Generated from data tables of MCNPX 2.5.0
 - ✗ Discretization effects
 - ✓ Validated with experimental measurements in the 4 – 3000 GeV energy range
- Nucl. Part. Phys. 10 (1984) 1609*

Reyna parametrization:

arXiv:hep-ph/0604145

- ✓ Analytical formula from different measurements
- ✓ Valid in the 1 - 4000 GeV energy range

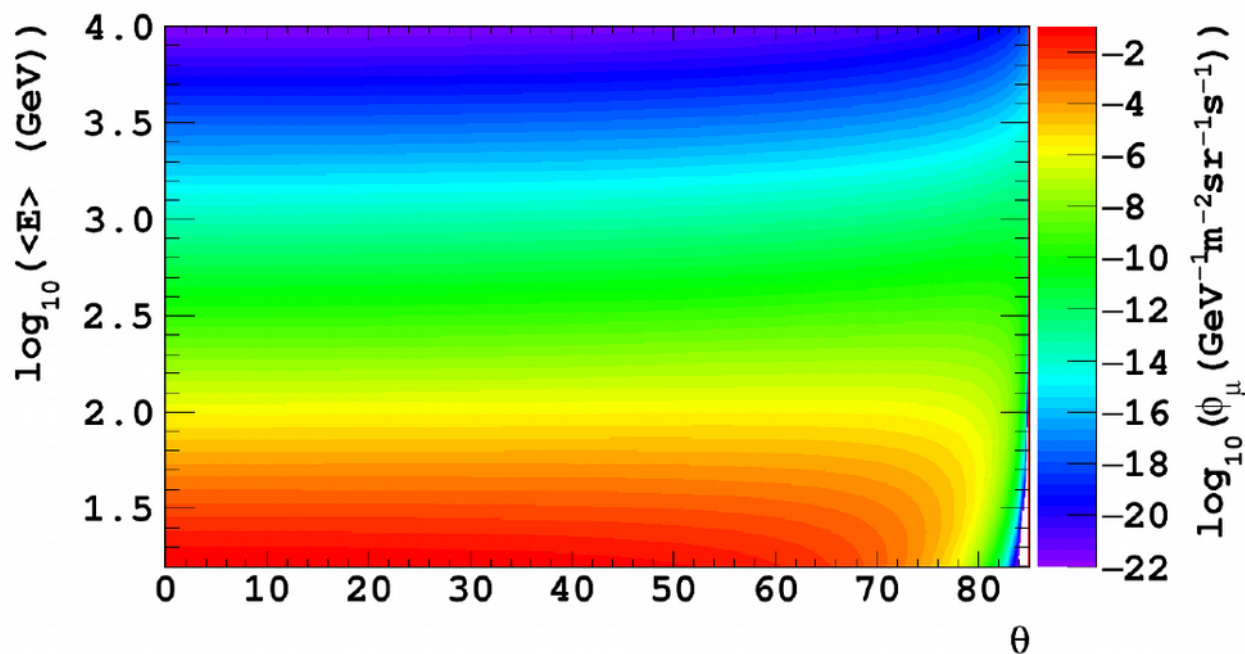
Simulations

- Due to the low overburden (120 and 300 m.w.e.) muons down to 20 and 40 GeV respectively are able to reach the detectors
 - It is for low energies where muon models present more differences
- Comparing simulations between them and w.r.t. experimental data would allow to validate these models

Extended Gaisser parametrization:

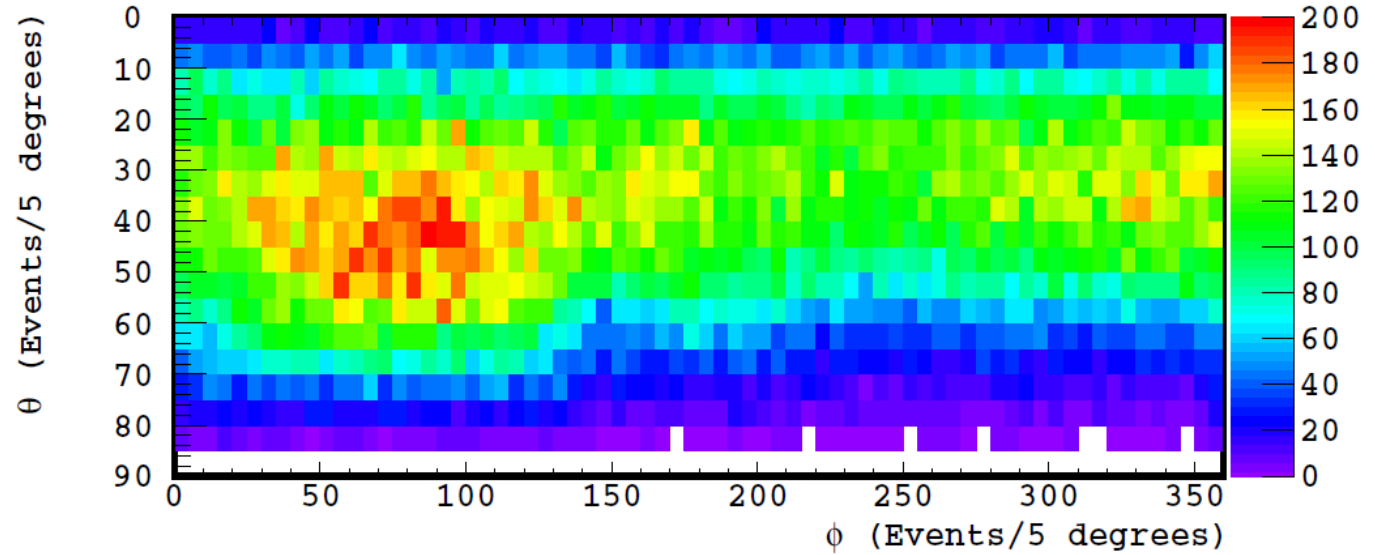
Phys. Rev. D 74 (2006) 053007

- ✓ Based on Gaisser analytical formula ($E_\mu > 100/\cos(\theta)$ GeV)
- Originally not valid for low energy; valid extension?

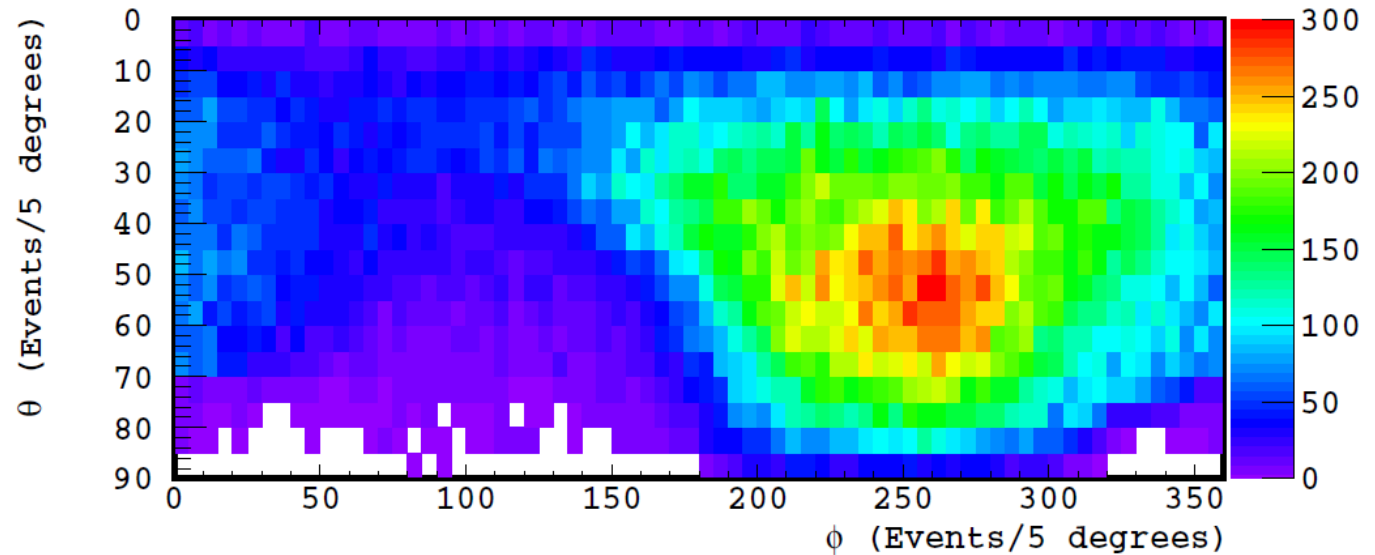


Simulations → Angular distributions

Near detector

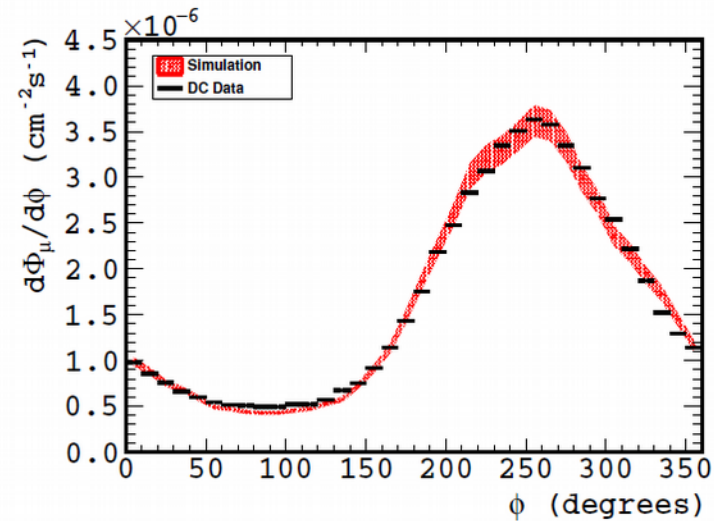
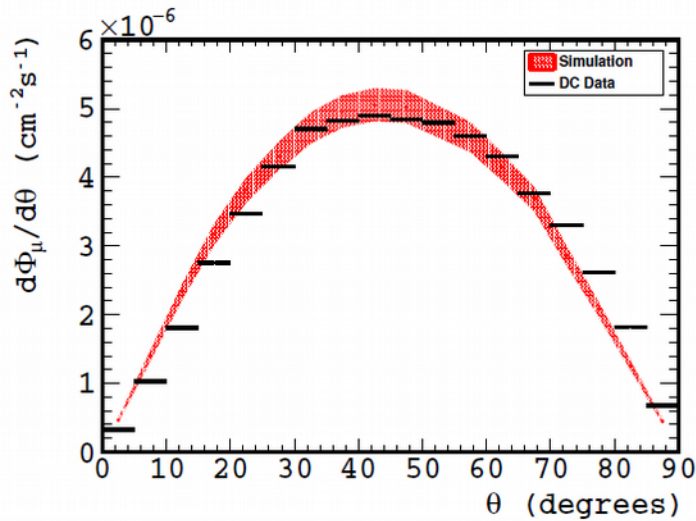


Far detector



Data / MC comparisons

Far detector



Data: $\phi_{\mu} = 7.00 \pm 0.05 \cdot 10^{-4} \text{ cm}^{-2} \text{ s}^{-1}$

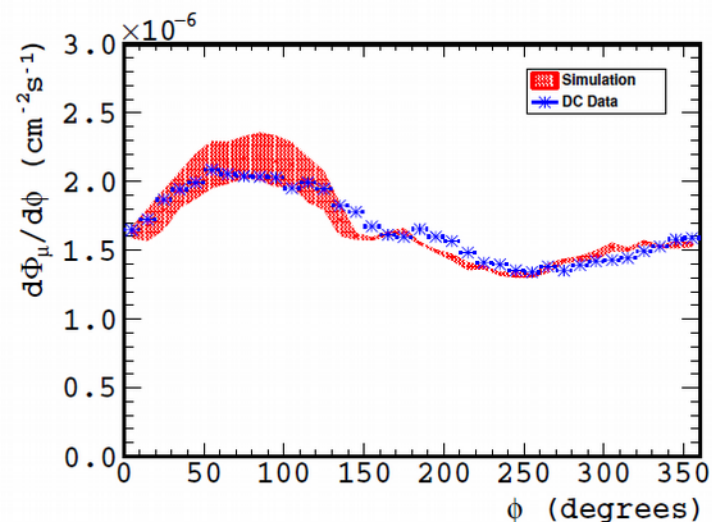
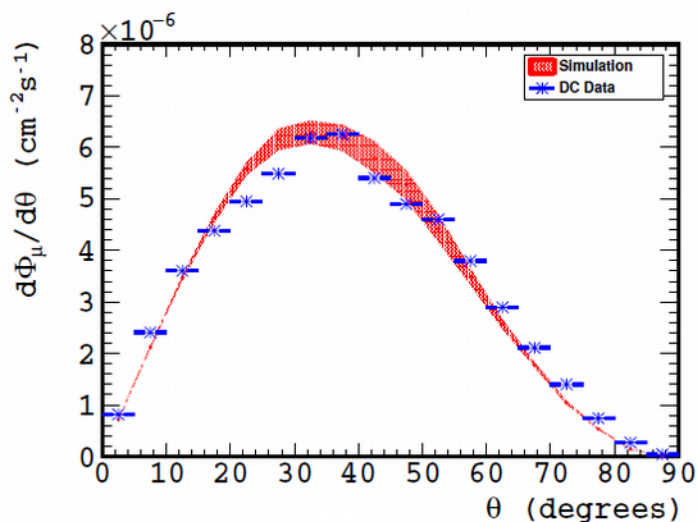
Simulations: $\phi_{\mu} = 7.24 \pm 0.33 \cdot 10^{-5} \text{ cm}^{-2} \text{ s}^{-1}$

In agreement within:

- Simulations precision (due to profile digitization)
- Track reconstruction algorithm accuracy

Data / MC comparisons

Near detector



Differences due to:

- Uncertainties in the low energy muon parametrization
- Is still valid the extended Gaisser parametrization?
- Lower precision in the profile digitization
- Inhomogeneities along the overburden?

Data: $\phi_{\mu} = 3.64 \pm 0.04 \cdot 10^{-4} \text{ cm}^{-2} \text{ s}^{-1}$

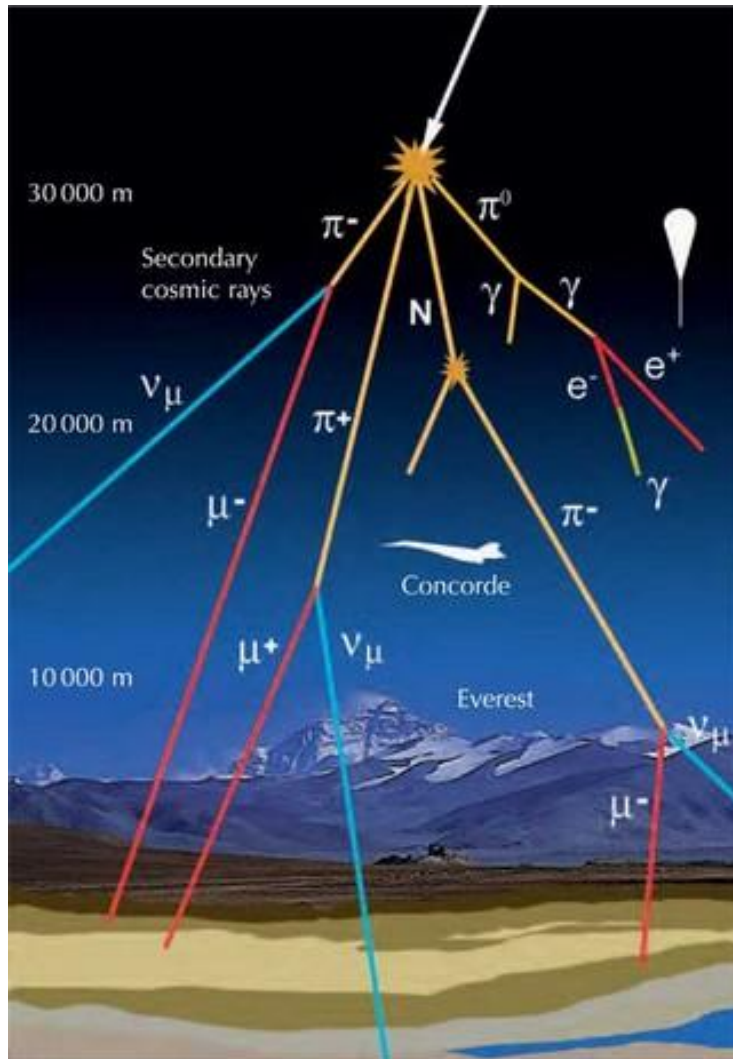
Simulations: $\phi_{\mu} = 3.47 \pm 0.12 \cdot 10^{-5} \text{ cm}^{-2} \text{ s}^{-1}$

- Even if (don't forget) **Double Chooz** was conceived as a **neutrino detection experiment**
- Muon characterization has revealed:
 - Muons are efficiently detected
 - Corresponding tracks has been successfully reconstructed
 - Simulation framework has been performed and cross-checked with experimental data
 - Overall agreement
- Moreover:
 - Double Chooz has been (it is being actually) operated from 2011 → High muon statistics
 - Simulation provides additional information not available from experimental data



**More Physics
is possible...**

- Annual modulation on the detected muon flux is expected:



- Fraction of mesons decaying to muons depends on the air density:

→ **Higher temperature**

→ Lower density

→ Mesons mean free path longer

→ Higher fraction of mesons decaying (to muons) before interacting

→ **Higher muon rate**

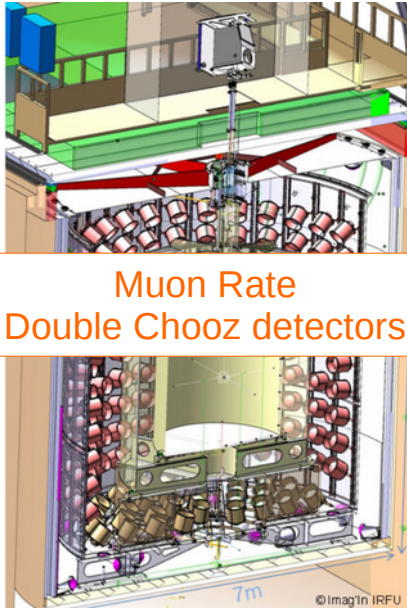
- $p + N \rightarrow$ Mesons (mostly π but also K)

↳ Decay to muons $\tau_{\pi(K)} = 26.0$ (12.4) ns

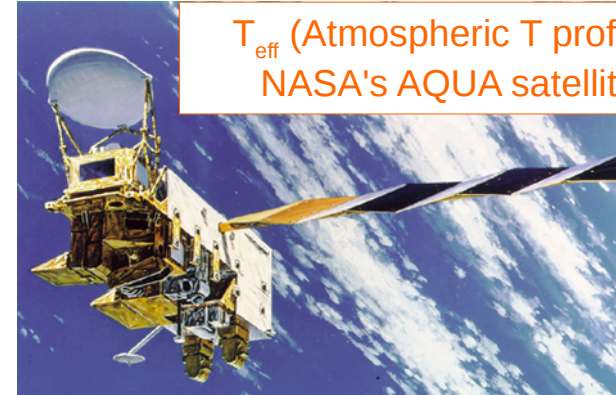
- Muons lose energy along their path through the atmosphere (and the rock over the detector)

- Deeper detectors** → **Higher E_μ required**

- Ingredients to study the annual modulation:



Muon Rate
Double Chooz detectors



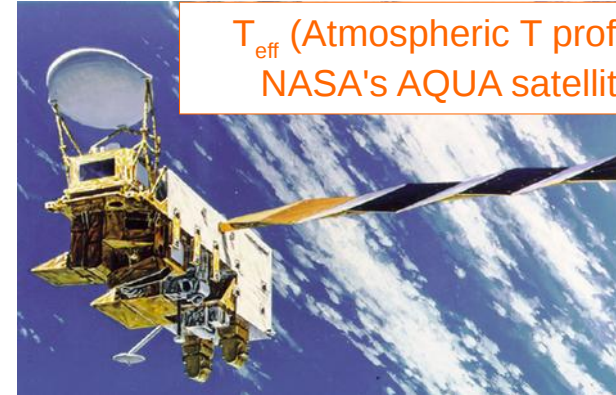
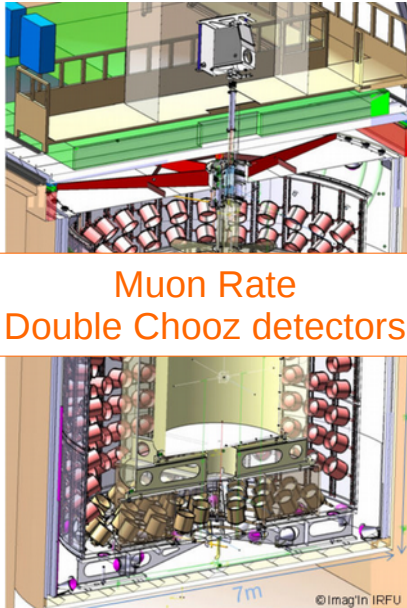
T_{eff} (Atmospheric T profile)
NASA's AQUA satellite

$$T_{\text{eff}} = \frac{\sum_{n=0}^{N-1} \Delta X_n \cdot T(X_n)(W_{\pi}(X_n) + W_K(X_n))}{\sum_{n=0}^N \Delta X_n (W_{\pi}(X_n) + W_K(X_n))}$$

$$W_{\pi,K}(X) = \frac{(1 - X/\Lambda'_{\pi,K})^2 e^{-X/\Lambda_{\pi,K}} A_{\pi,K}^1}{\gamma + (\gamma + 1) B_{\pi,K}^1 K_{\pi,K}(X) (\langle E_{\text{thr}} \cos \theta \rangle / \epsilon_{\pi,K})^2}$$

$$K_{\pi,K}(X) = \frac{(1 - X/\Lambda'_{\pi,K})^2}{(1 - e^{-X/\Lambda'_{\pi,K}}) \Lambda'_{\pi,K} / X}$$

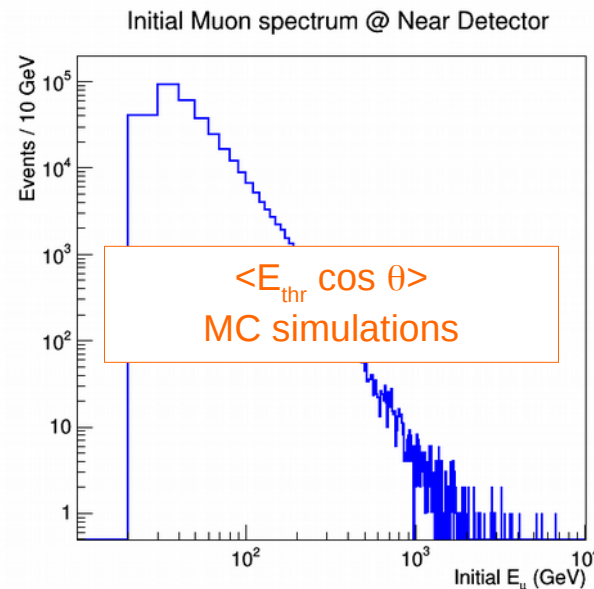
- Ingredients to study the annual modulation:



$$T_{\text{eff}} = \frac{\sum_{n=0}^{N-1} \Delta X_n \cdot T(X_n)(W_{\pi}(X_n) + W_K(X_n))}{\sum_{n=0}^N \Delta X_n (W_{\pi}(X_n) + W_K(X_n))}$$

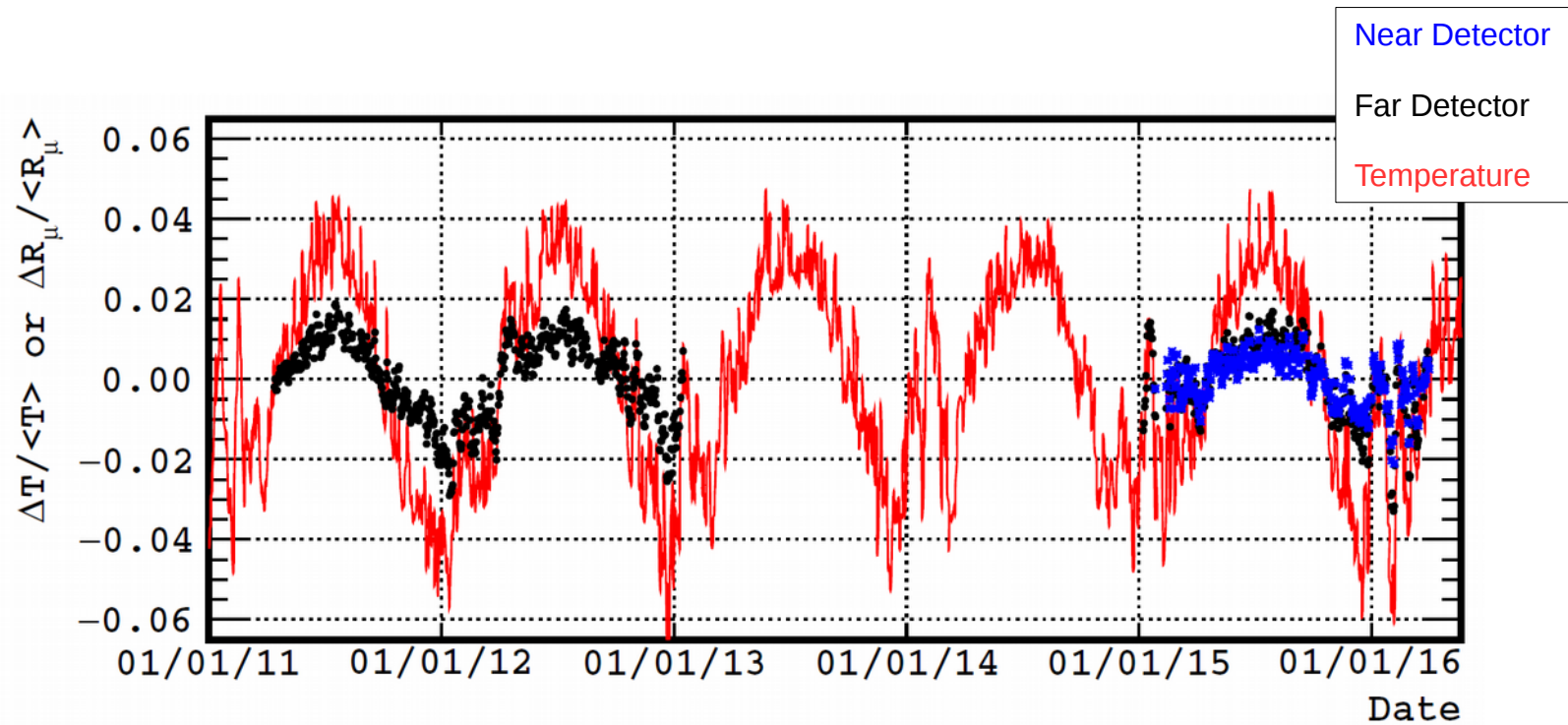
$$W_{\pi,K}(X) = \frac{(1 - X/\Lambda'_{\pi,K})^2 e^{-X/\Lambda_{\pi,K}} A_{\pi,K}^1}{\gamma + (\gamma + 1) B_{\pi,K}^1 K_{\pi,K}(X) \langle E_{\text{thr}} \cos \theta \rangle \epsilon_{\pi,K}^2}$$

$$K_{\pi,K}(X) = \frac{(1 - X/\Lambda'_{\pi,K})^2}{(1 - e^{-X/\Lambda'_{\pi,K}}) \Lambda'_{\pi,K}/X}$$



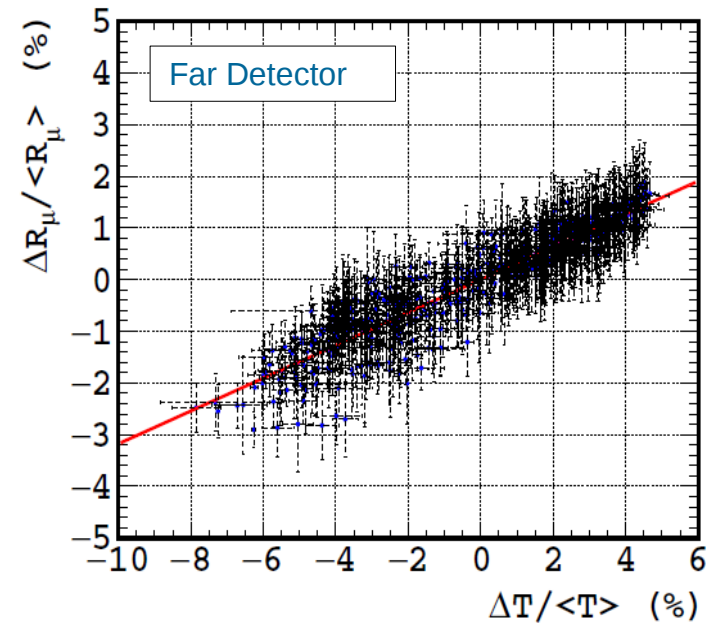
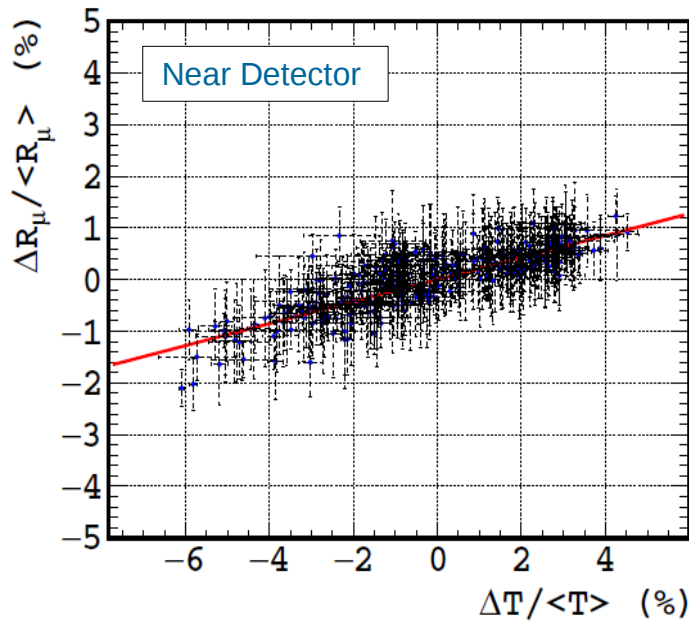
$$\langle E_{\text{thr}} \cos \theta \rangle = \int_{\theta=0}^{\pi/2} E_{\text{thr}}(\theta) \Phi_{\text{norm}}^{\mu}(\theta) \cos \theta d\theta$$

Near detector	$\langle E_{\text{thr}} \cos \theta \rangle = 22.3 \pm 4.8 \text{ GeV}$
Far detector	$\langle E_{\text{thr}} \cos \theta \rangle = 46.0 \pm 10.0 \text{ GeV}$



Effective temperature coefficient (α_T) :

$$\frac{\Delta R_\mu}{\langle R_\mu \rangle} = \alpha_T \frac{\Delta T_{eff}}{\langle T_{eff} \rangle}$$



Effective temperature coefficient (α_T) :

Near detector: $\alpha_T = 0.212 \pm 0.013$ (stat) ± 0.011 (sys)

Correlation (R_μ, T_{eff}) = 0.855

Far detector: $\alpha_T = 0.355 \pm 0.002$ (stat) ± 0.017 (sys)

Correlation (R_μ, T_{eff}) = 0.923

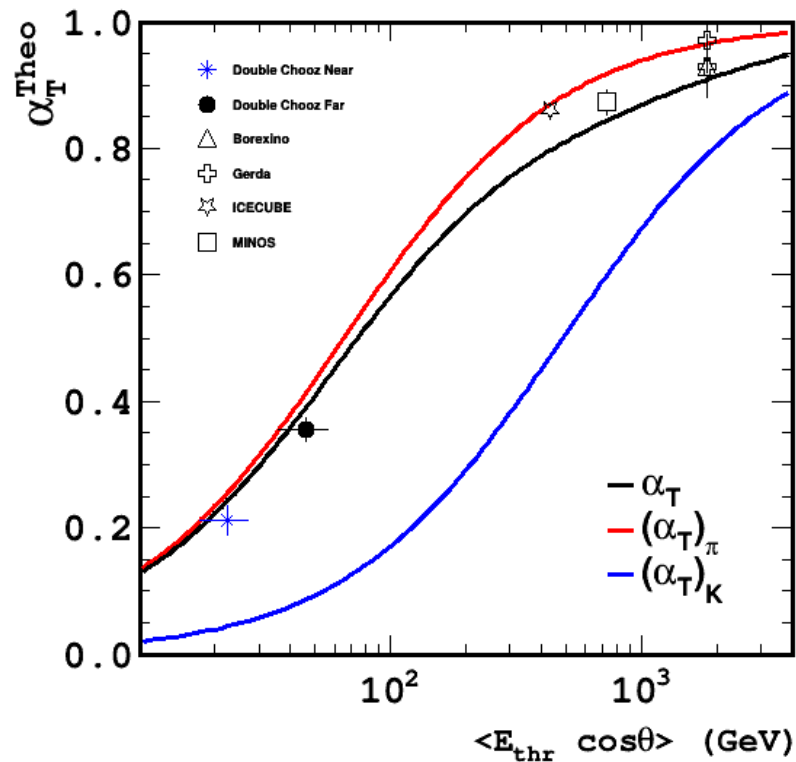
- Double Chooz results for α_T can be used to compare / validate theoretical models

$$\alpha_T^{\text{Theo}} = \frac{1}{D_\pi} \frac{1/\epsilon_K + A_K^1 (D_\pi/D_K)^2/\epsilon_\pi}{1/\epsilon_K + A_K^1 (D_\pi/D_K)/\epsilon_\pi}$$

$$D_{K,\pi} = \frac{\gamma}{\gamma + 1} \frac{\epsilon_{K,\pi}}{1.1 \langle E_{\text{thr}} \cos \theta \rangle} + 1$$

It depends, via A_K^1 , of the assumed Kaon to Pion ratio

$r_{K/\pi} = 0.149 \pm 0.060$ T.K. Gaisser, *Cosmic rays and particle physics*, Cambridge University Press, Cambridge U.K., (1990)



- Double Chooz measurements in agreement with theoretical model
- One of the first validations for low values of $\langle E_{\text{thr}} \cos \theta \rangle$

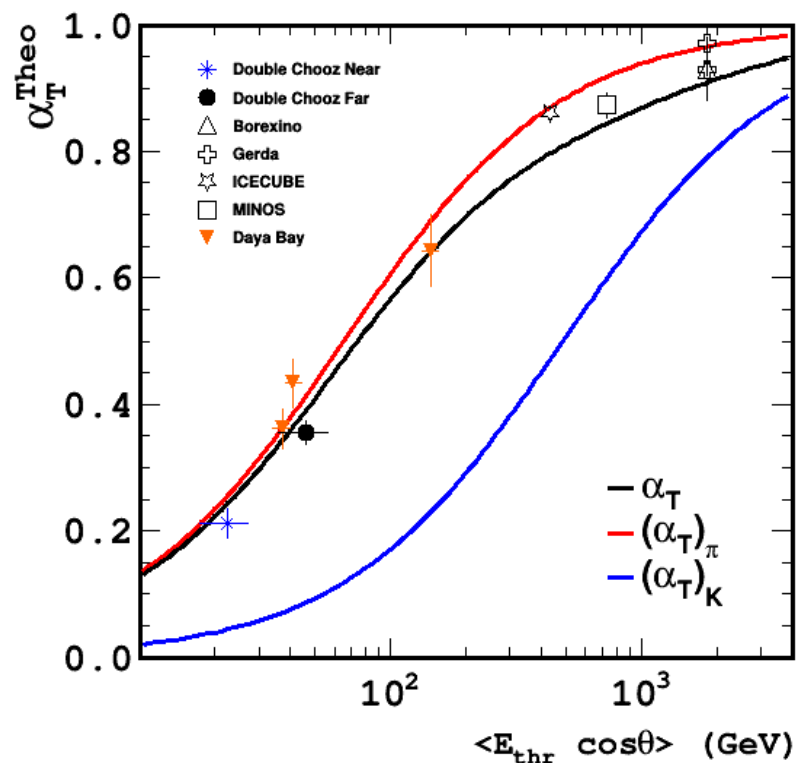
- Double Chooz results for α_T can be used to compare / validate theoretical models

$$\alpha_T^{\text{Theo}} = \frac{1}{D_\pi} \frac{1/\epsilon_K + A_K^1 (D_\pi/D_K)^2 / \epsilon_\pi}{1/\epsilon_K + A_K^1 (D_\pi/D_K) / \epsilon_\pi}$$

$$D_{K,\pi} = \frac{\gamma}{\gamma + 1} \frac{\epsilon_{K,\pi}}{1.1 \langle E_{\text{thr}} \cos \theta \rangle} + 1$$

It depends, via A_K^1 , of the assumed Kaon to Pion ratio

$r_{K/\pi} = 0.149 \pm 0.060$ *T.K. Gaisser, Cosmic rays and particle physics, Cambridge University Press, Cambridge U.K., (1990)*



- Double Chooz measurements in agreement with theoretical model
- One of the first validations for low values of $\langle E_{\text{thr}} \cos \theta \rangle$
- Trigger for equivalent studies for other reactor ν experiments
 - Daya Bay \rightarrow JCAP 01 (2018) 001

Taking advantage of muons

- Atmospheric muons as radioactive source:
 - ✓ Natural – Non risky for health
 - ✓ Free
 - Rather intense
 - ✓ Extended and deep penetrating
 - Fairly well understood and parametrized



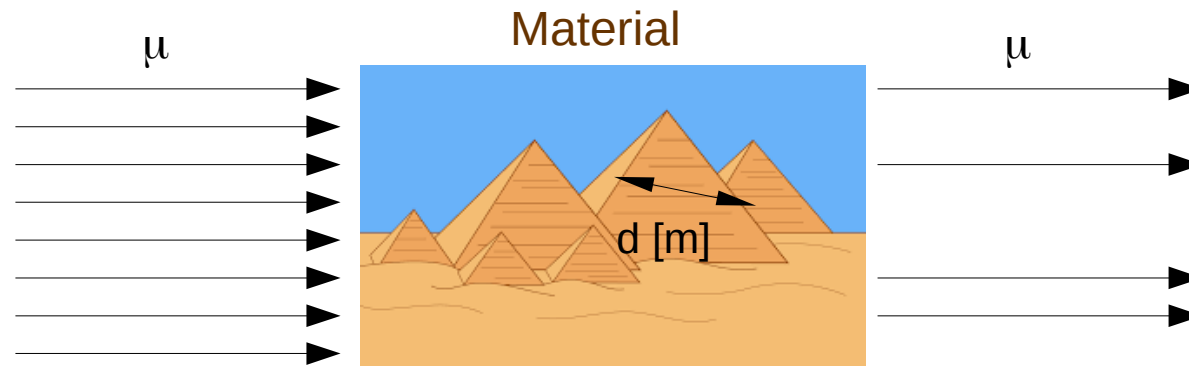
**Even More Physics
is possible...**

**More Physics
is possible...**



Initial flux ϕ_i

Basically dependant on the μ energy and zenith angle (E, θ)



Density: ρ [g/cm³]

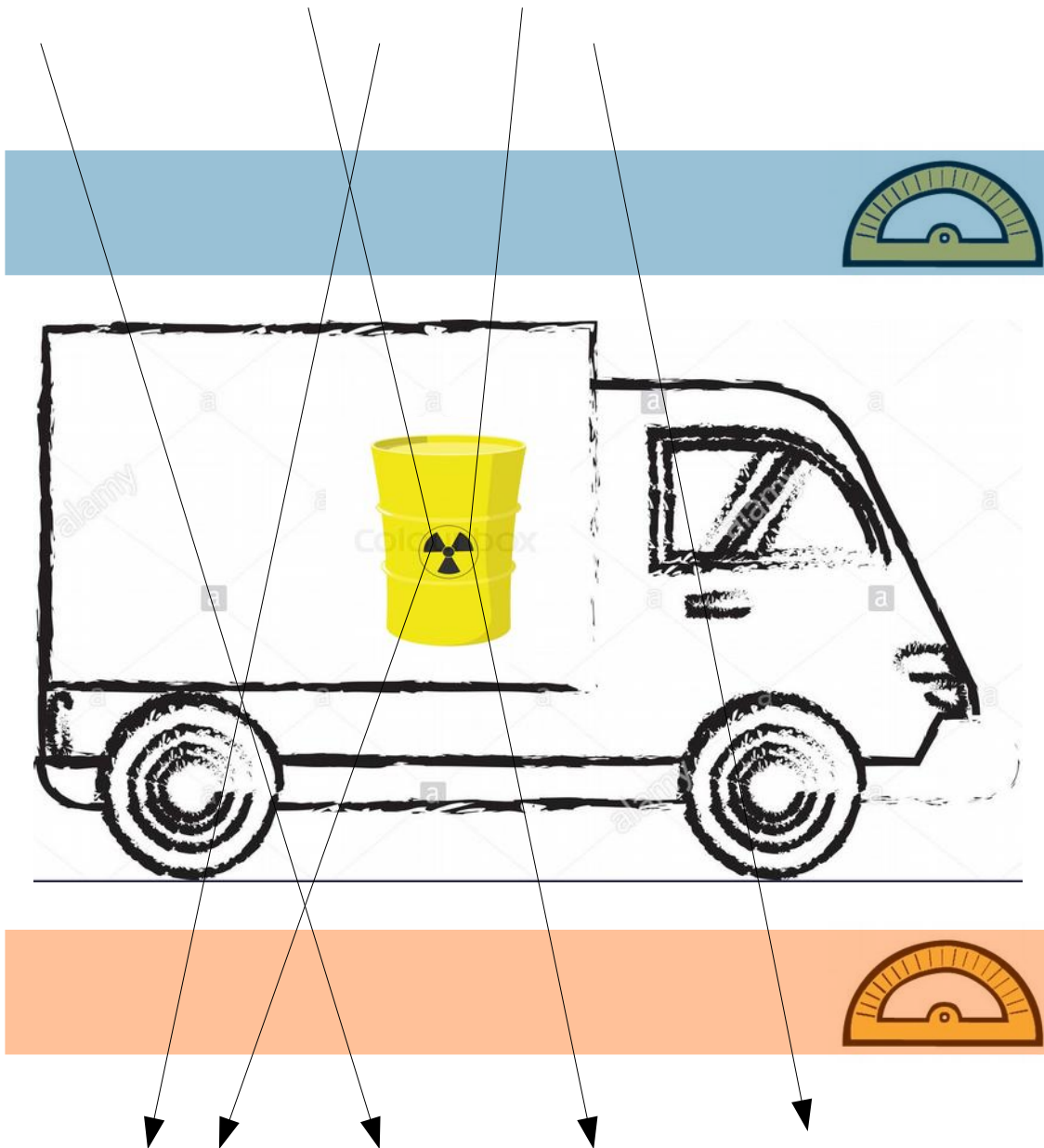
Opacity: δ [g/cm²] = ρd



Final flux ϕ_f

Detected muons for a given direction

- Ratio between initial and final fluxes is directly related with Opacity
- Differences in final flux (after normalization) for different directions also points to Opacity differences



- Muon trajectory deviation is related with the material density (Moliere Theory)
 - Comparing *initial* vs *final* directions for each point of the studied object, a mean deviation angle can be obtained, then a density map.
- ✓ Faster
- ✓ For smaller objects with no big opacities

- 1955: Study of the rock overburden over a tunnel in Australia
 - *E.P. George, Cosmic rays measure overburden of tunnel, Commonwealth Engineer 455 (1955)*
- **1970: L.W. Alvarez (1968 Physics Nobel Prize)**
 - Scanning of Chephren Pyramid looking for internal vaults
 - Nothing found
 - *Alvarez, L.W. (1970). "Search for hidden chambers in the pyramids using cosmic rays". Science 167: 832*

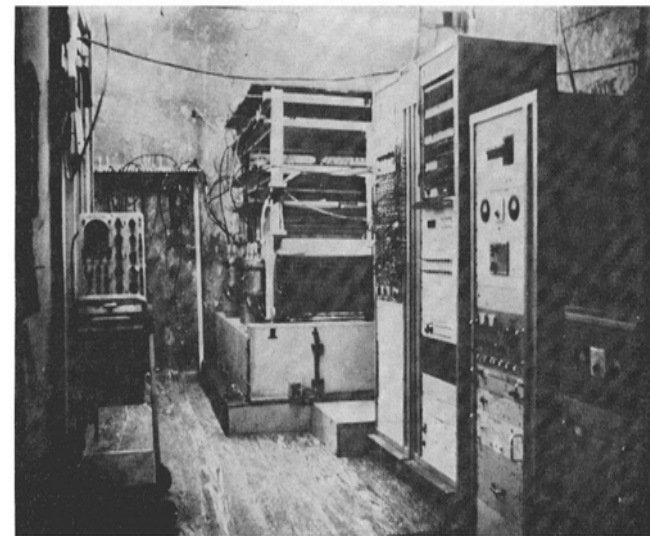
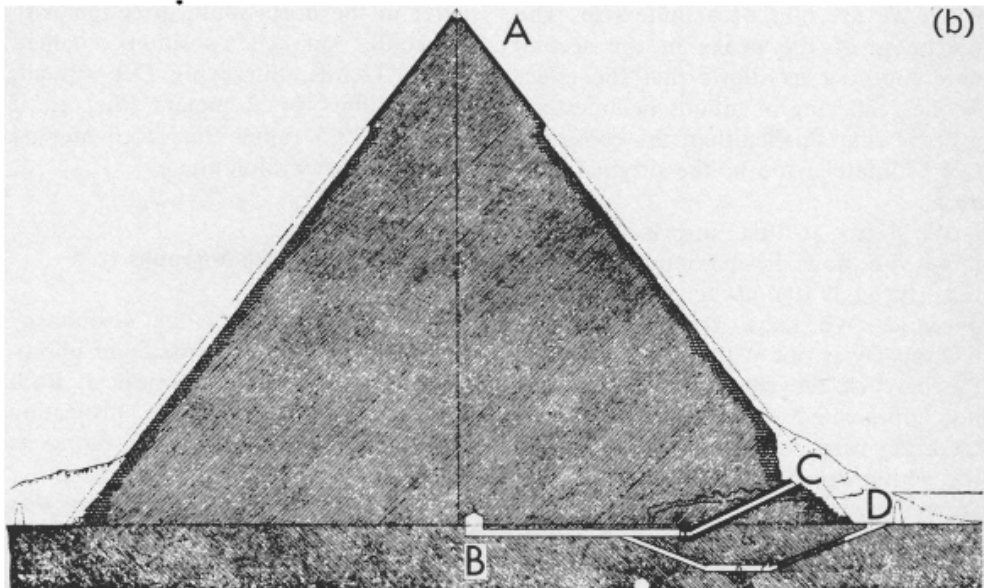
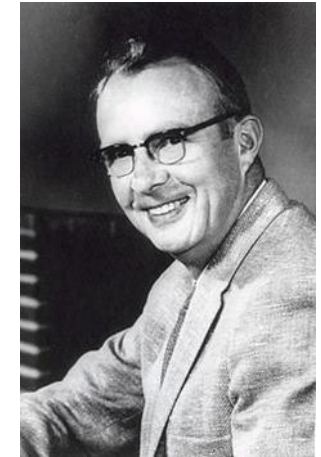
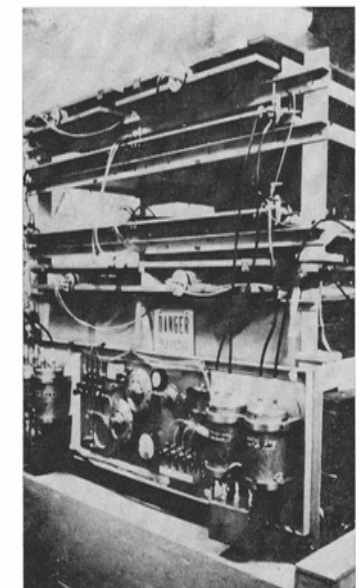
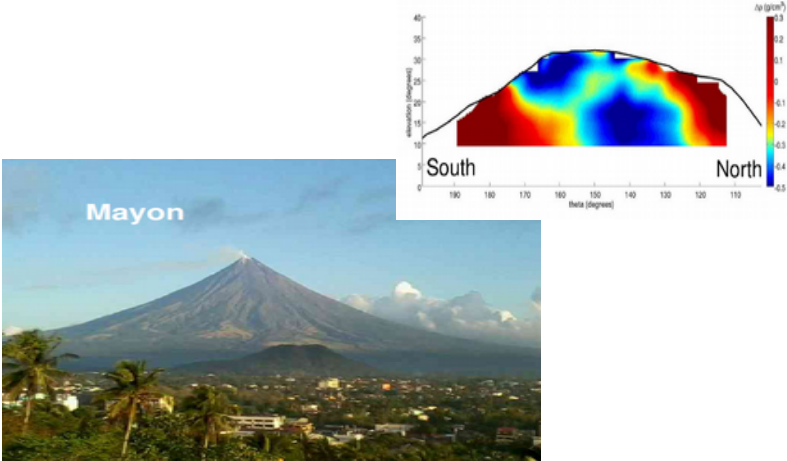


Fig. 6 (left). The equipment in place in the Belzoni Chamber under the pyramid.
Fig. 7 (right). The detection apparatus containing the spark chambers.



Transmission

Deviation



Mayon

Volcano Tomography



Archeology

The 'Transmission' section features two images. The top image shows the Mayon volcano with a muon tomography plot overlaid, displaying a color-coded cross-section of the volcano's interior. The plot has a vertical axis for altitude (0 to 40) and a horizontal axis for theta (190 to 110). A color scale on the right indicates muon flux density from 0.4 to 0.3. The bottom image shows the Great Pyramids of Giza with a similar muon tomography plot overlaid, showing the internal structure of the pyramids.



Fukushima scanning

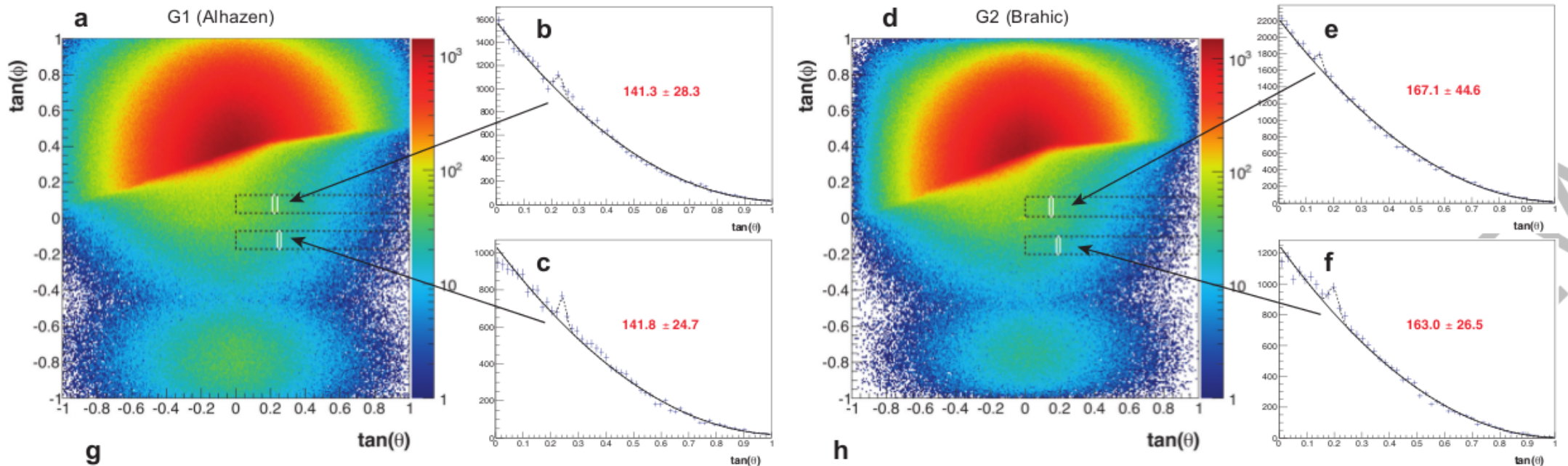
Nuclear control and safety



Homeland security

The 'Deviation' section features two images. The top image shows the Fukushima nuclear power plant with a muon tomography scan overlaid, displaying a dark, circular scan area. The bottom image shows a truck being scanned by a muon tomography system, with a diagram illustrating the detector setup and the scanning process. The diagram shows a truck with a 'Scanner' and 'Engine' on top, and 'Detectors' on the sides. Red arrows indicate muon paths, with labels for 'Large scattering', 'Miss scattering', and 'Hit scattering'.

- **Simulations** represent a **useful tool** in muon tomography to:
 - Perform feasibility studies
 - Choose best detector position
 - Data analysis and interpretation
- } Improve measurement sensitivity
- To achieve that, the simulation framework **requires**:
 - The precise implementation of :
 - The studied geometry
 - The muon parametrization at Earth surface
 - Consider all the muon physics process
 - Definition of the used detector features and performance



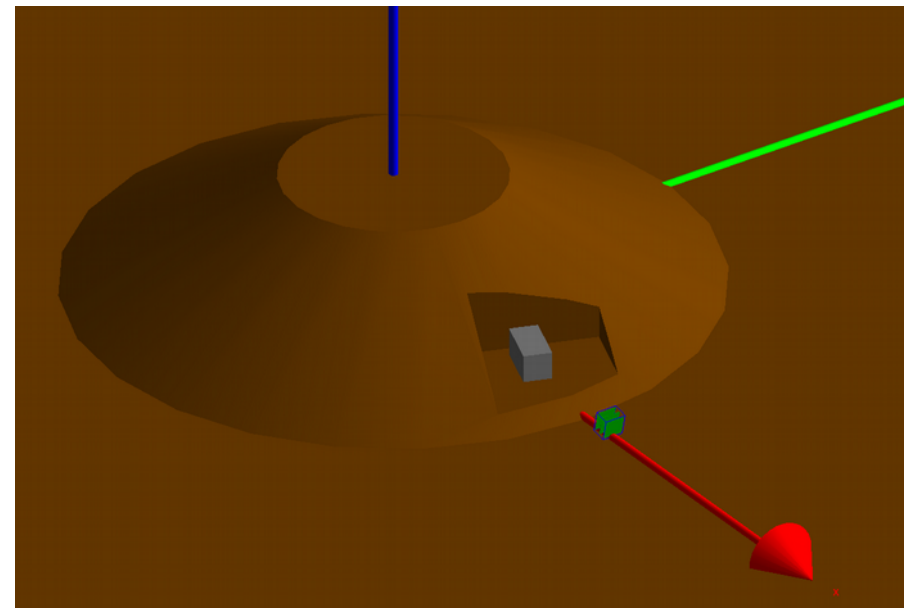
- Outstanding (Nature indeed) result taking advantage of:
 - State-of-the-art detector technology
 - Size of the “anomaly”
 - ~30 m over ~100 m of muon path across the pyramid
 - Position of the “anomaly”
 - Zenith angle anomaly – detector ~60° → Not optimal but still considerable muon flux

Example: Scanning of the Apollonia Macedonian Tumulus (Greece).
Feasibility study of a transmission measurement.

- **Tumulus:**

- Top $\varnothing = 32$ m; Base $\varnothing = 92$ m
- Height = 17 m
- Made of Soil with a Rock-wall chamber

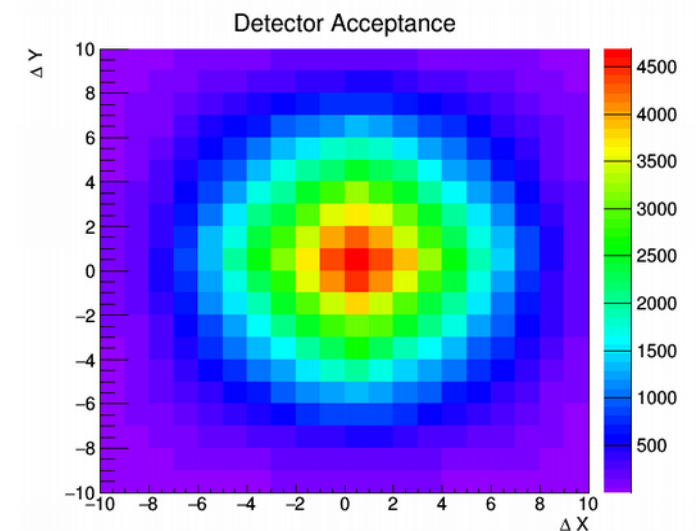
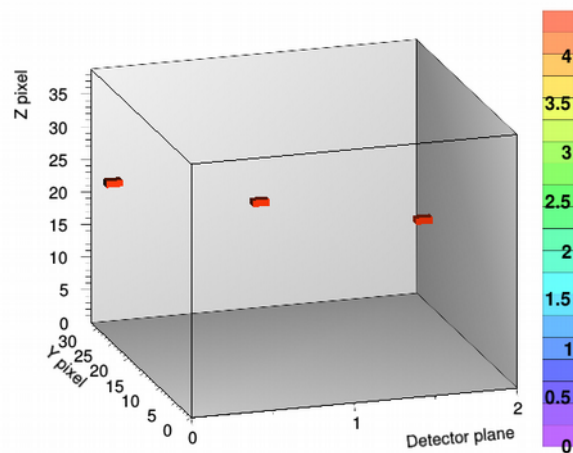
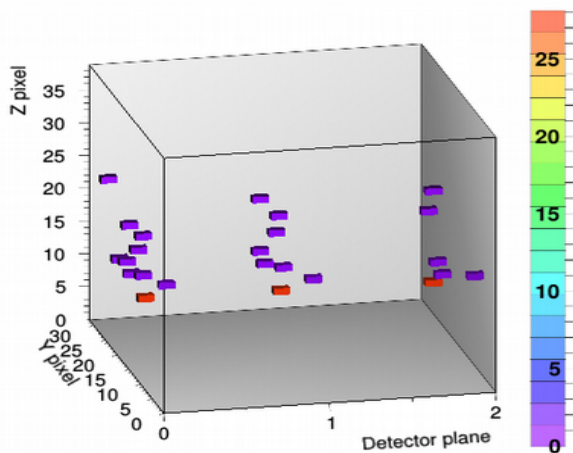
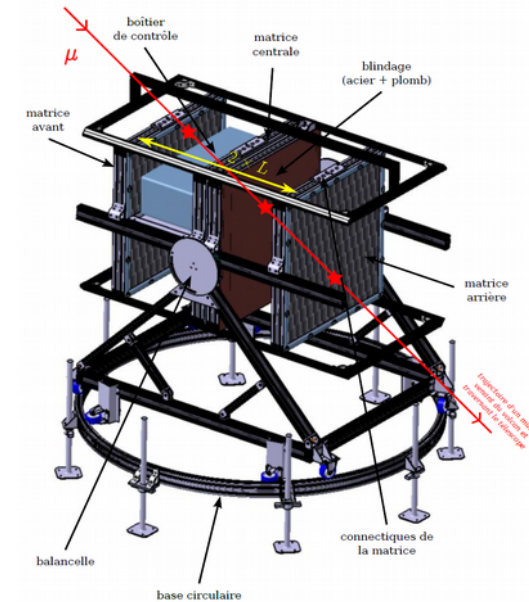
Incident $\theta = [70 - 80]^\circ$
Anomaly $\sim 10/100$ m



Example: Scanning of the Apollonia Macedonian Tumulus (Greece).
Feasibility study of a transmission measurement.

- Detector:**

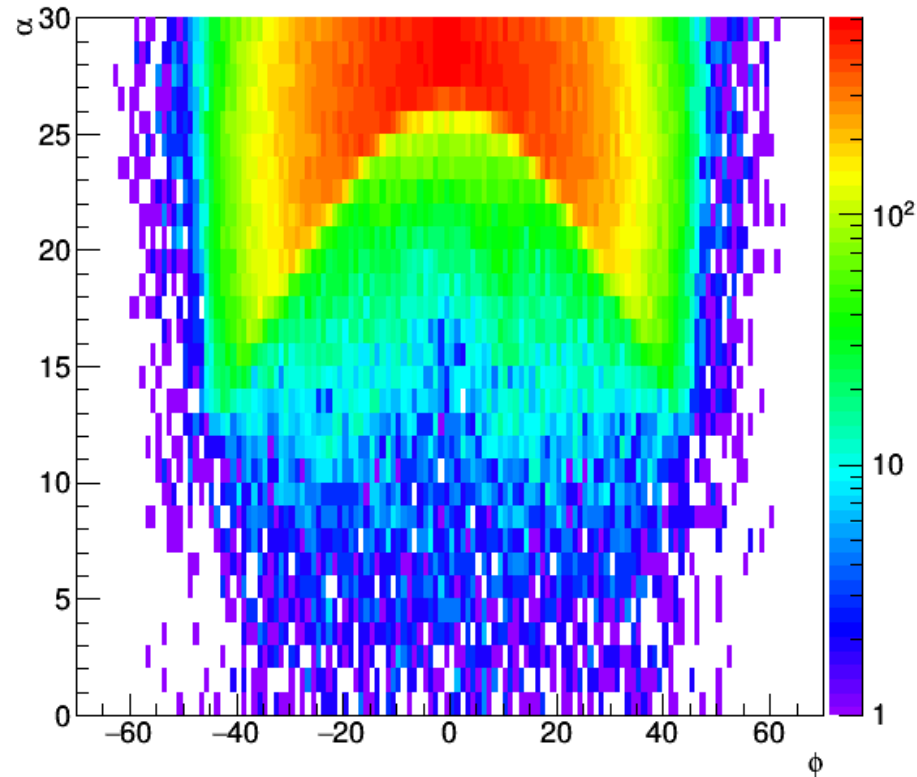
- Muon telescope based on plastic scintillators
- Evolution of those already used for volcanoes scanning
- Assumed angular resolution 1°



Example: Scanning of the Apollonia Macedonian Tumulus (Greece).
Feasibility study of a transmission measurement.

- Results:**

Angular distribution at detector

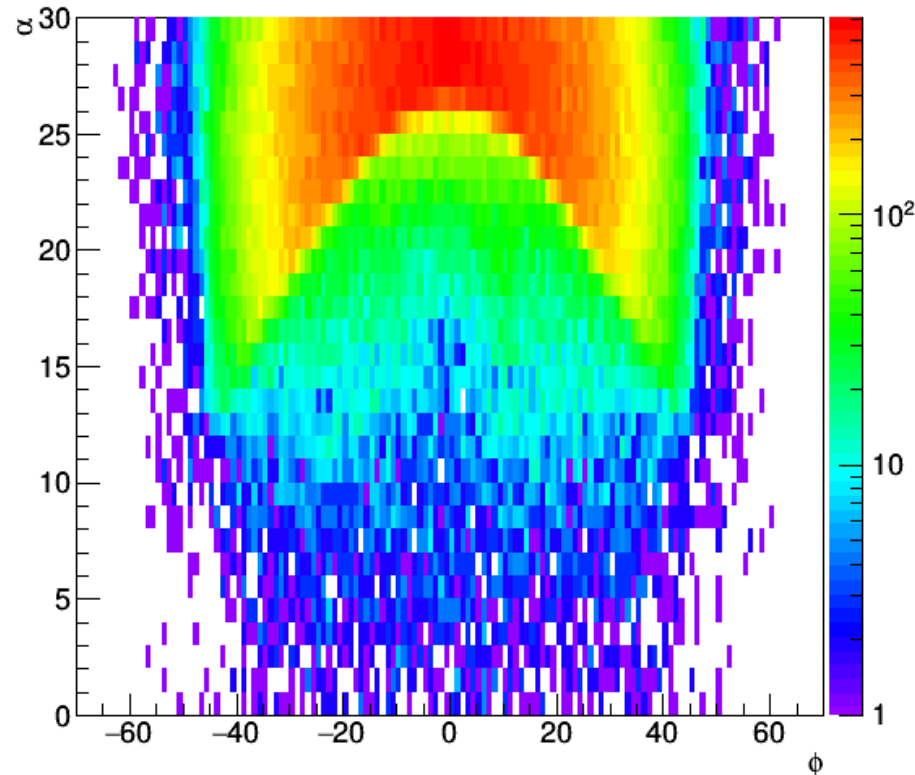


Raw results

Example: Scanning of the Apollonia Macedonian Tumulus (Greece).
Feasibility study of a transmission measurement.

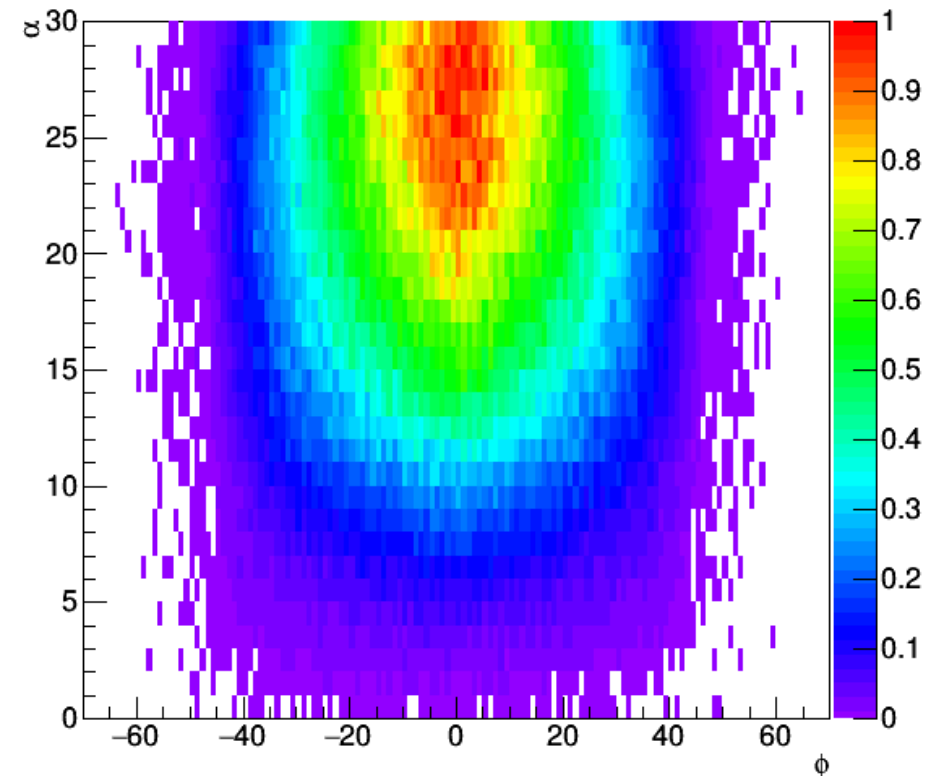
- Results:**

Angular distribution at detector



Raw results

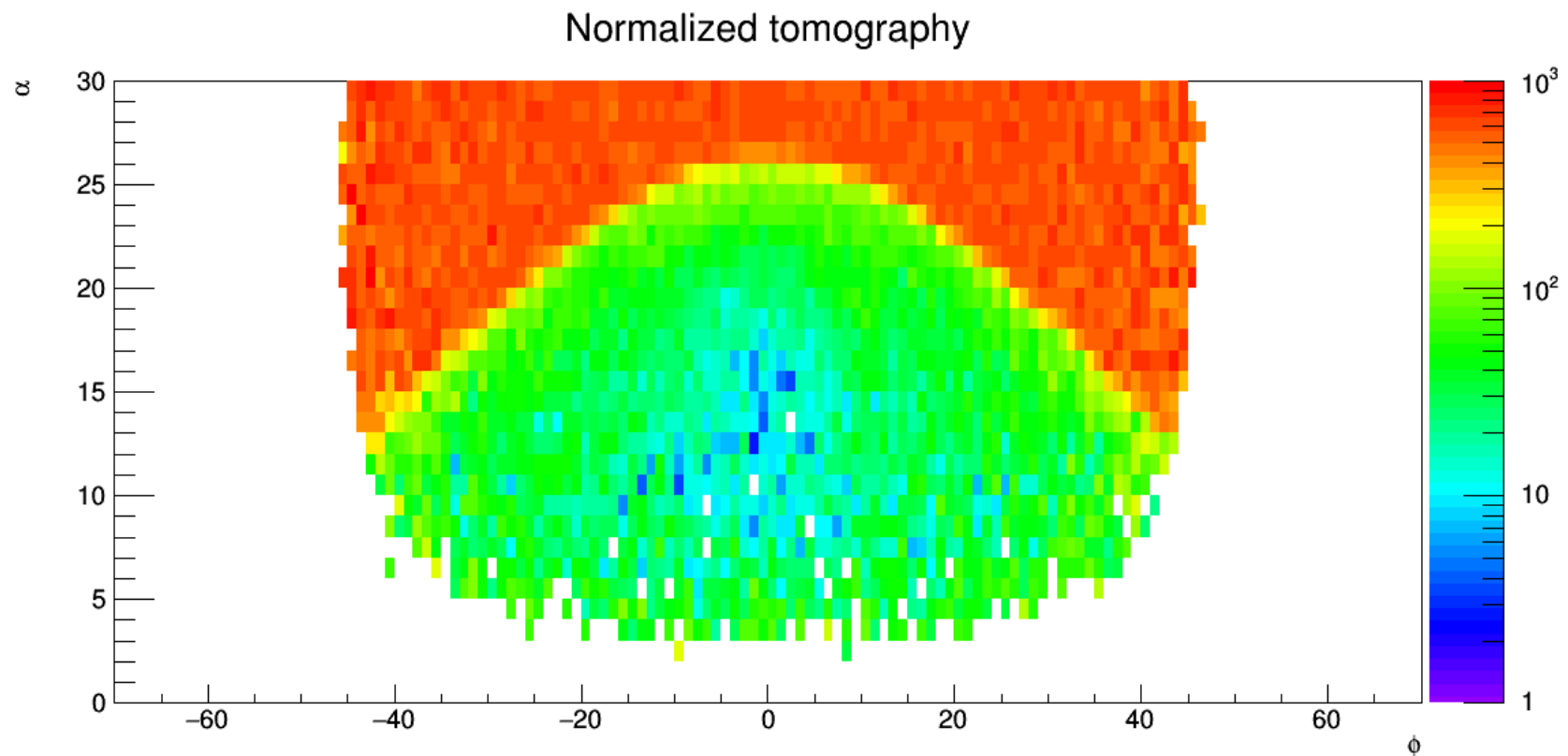
Detector response @ open air



Normalized results at open air with
the same inclination

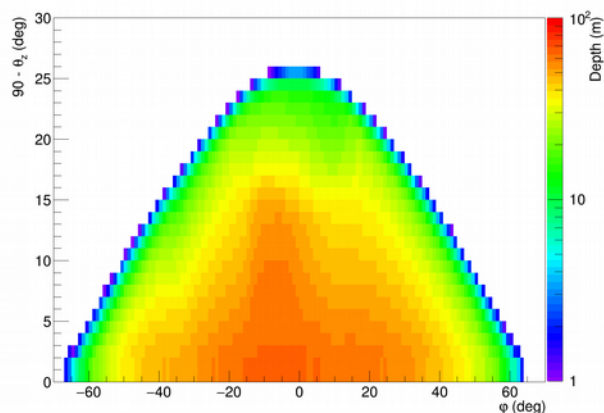
Example: Scanning of the Apollonia Macedonian Tumulus (Greece).
Feasibility study of a transmission measurement.

- Results:**



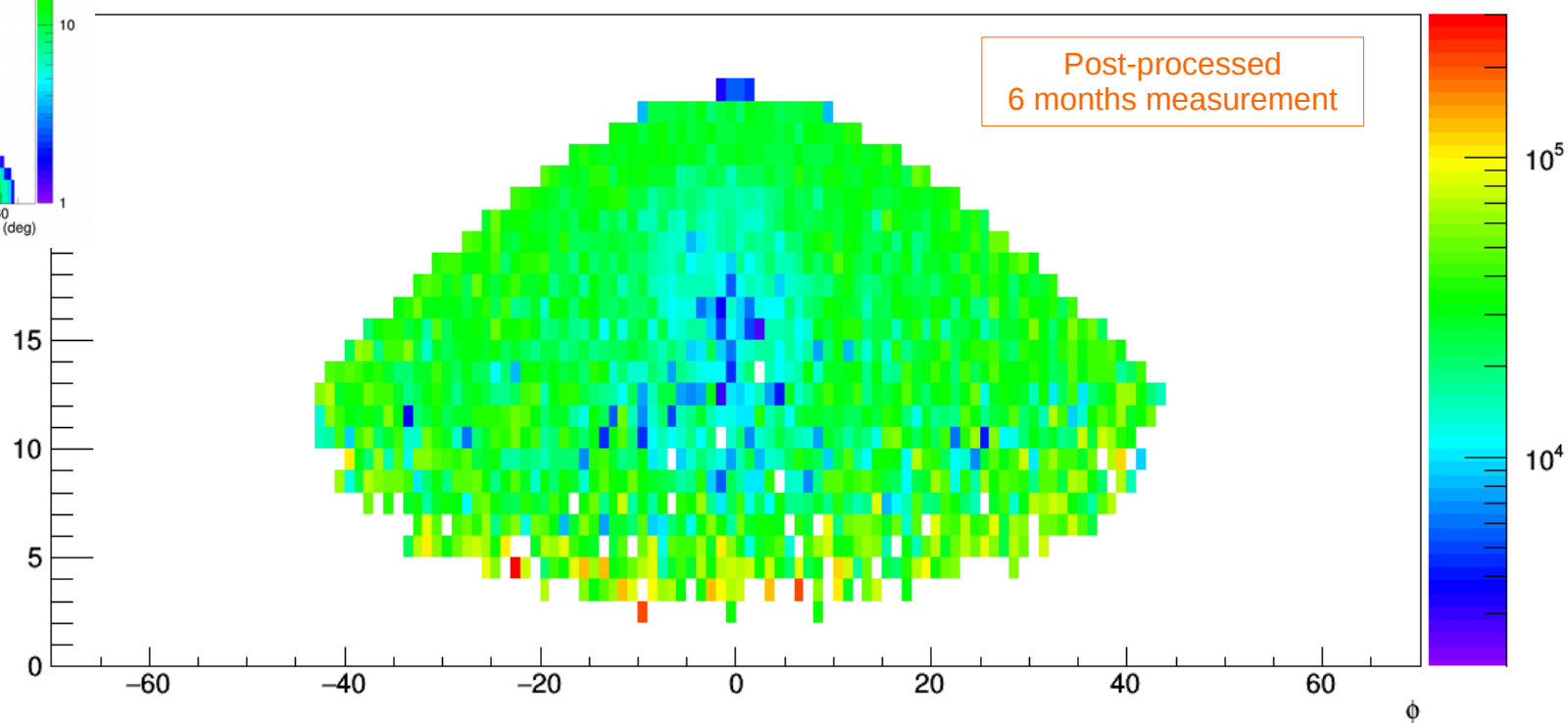
Example: Scanning of the Apollonia Macedonian Tumulus (Greece).
Feasibility study of a transmission measurement.

- Results:**



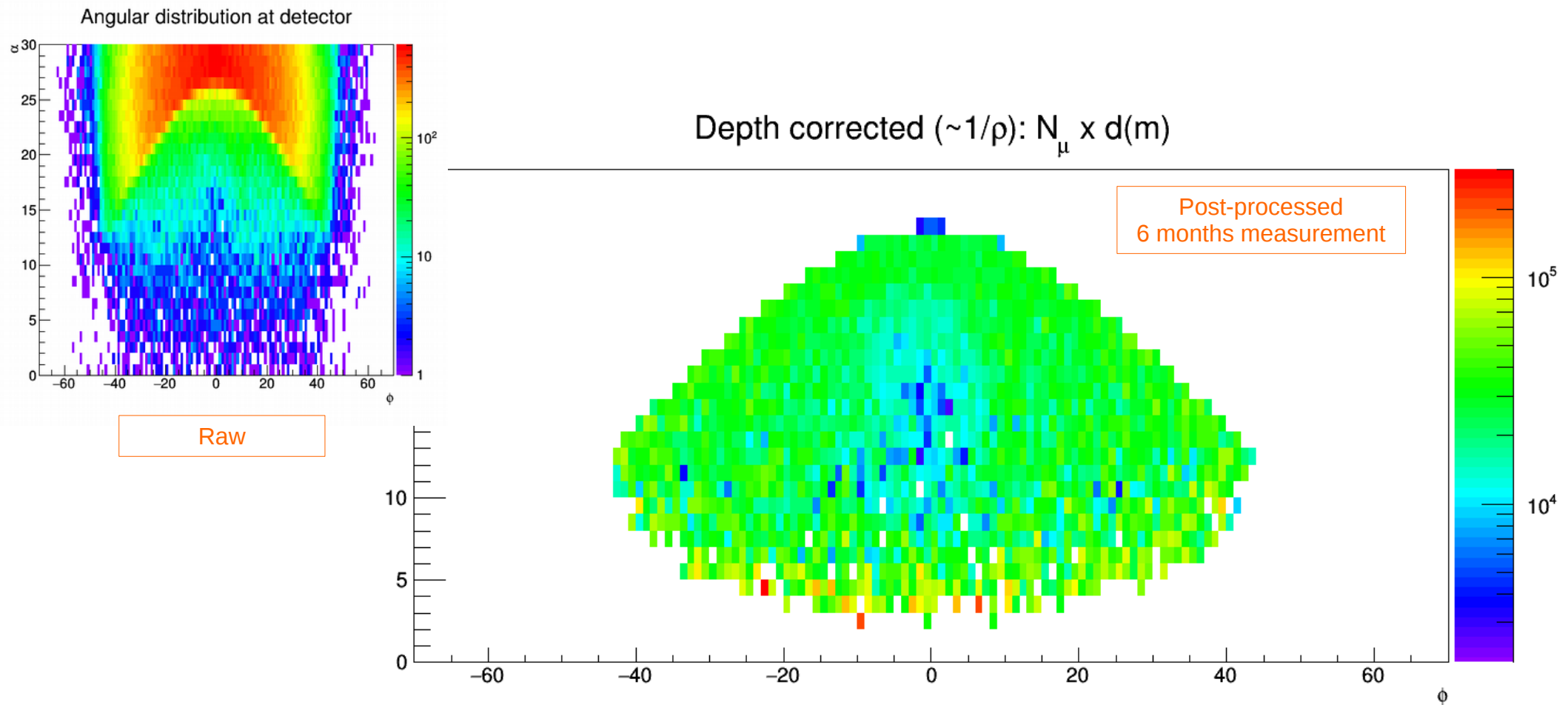
External shape

Depth corrected ($\sim 1/\rho$): $N_\mu \times d(m)$



Example: Scanning of the Apollonia Macedonian Tumulus (Greece).
Feasibility study of a transmission measurement.

- Results:**



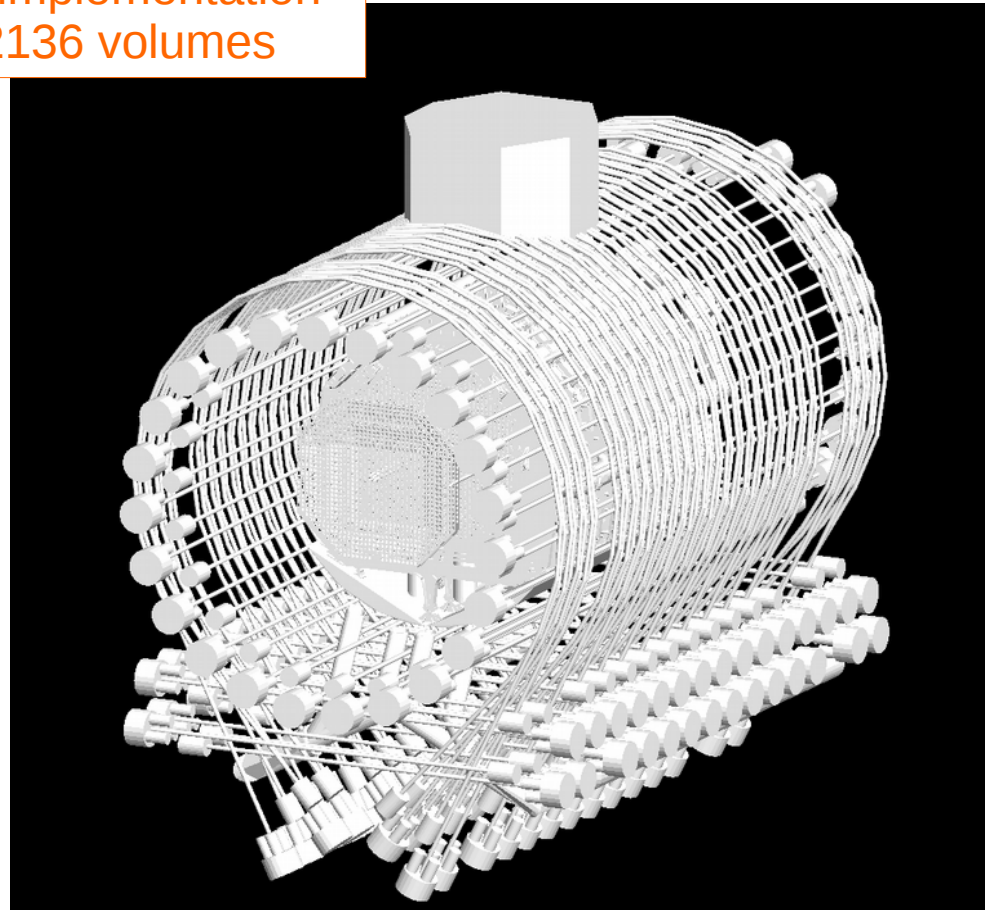
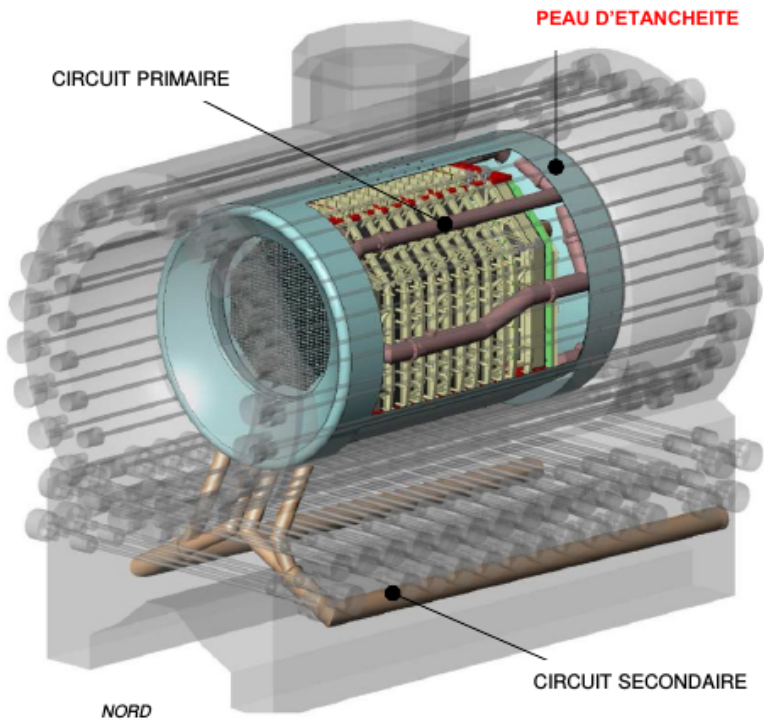
Towards high precision simulations: Implementation of geometries

From CAD designs

From objects 3D models: Topography, photo-grammetry...

G2-G3 reactors
CEA-Marcoule

G4 implementation
22136 volumes



CAD design composed by 866 different components

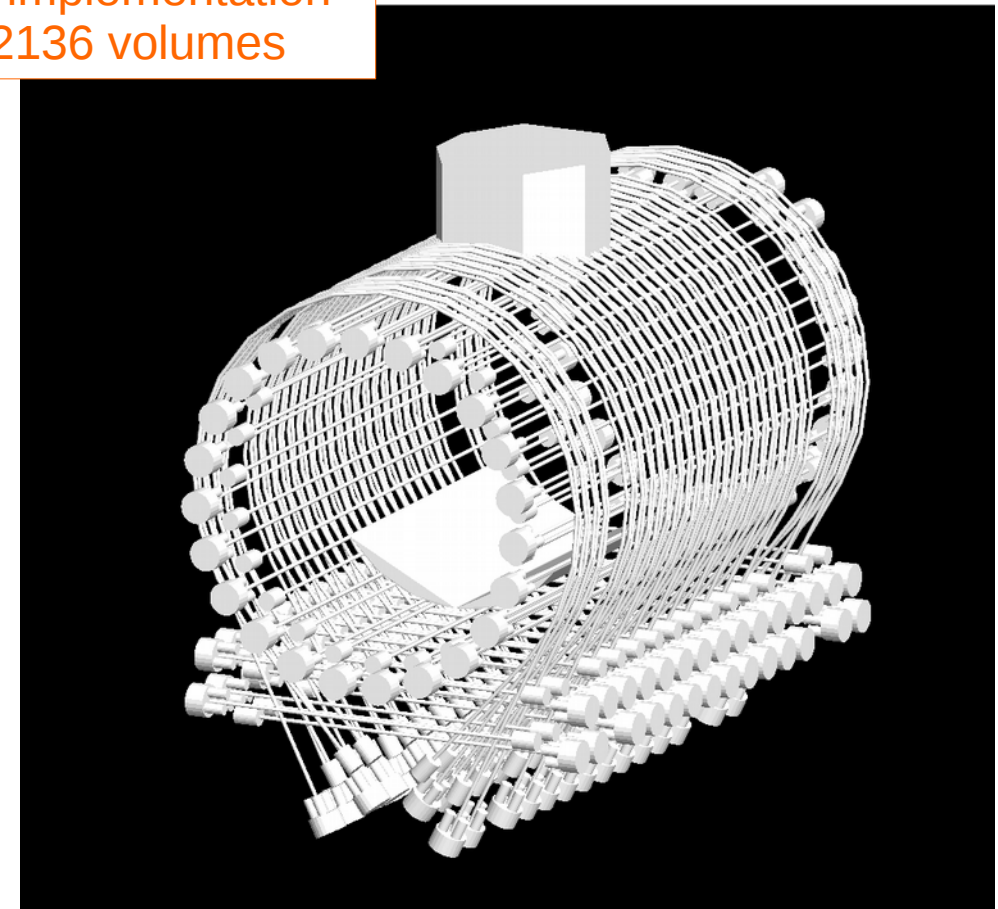
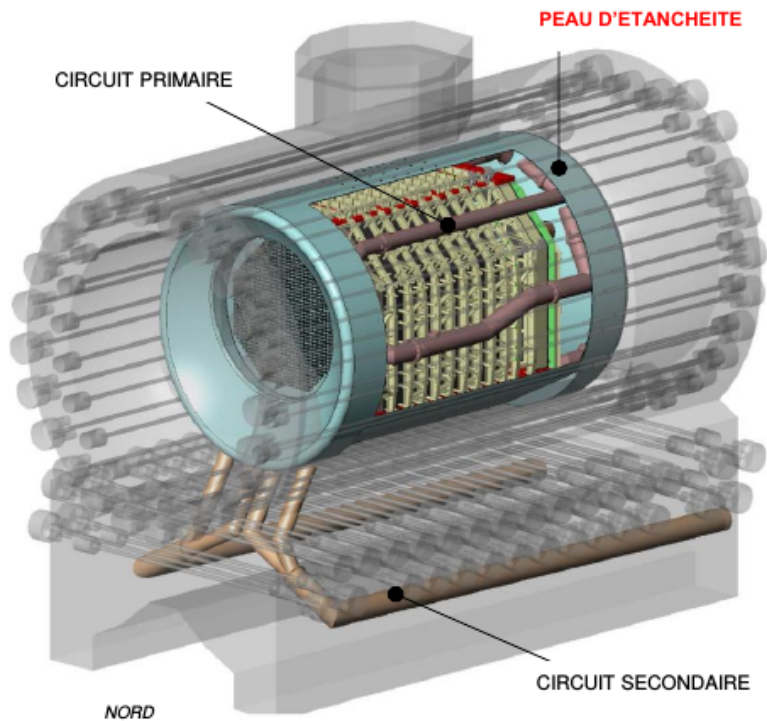
Towards high precision simulations: Implementation of geometries

From CAD designs

From objects 3D models: Topography, photo-grammetry...

G2-G3 reactors
CEA-Marcoule

G4 implementation
22136 volumes



CAD design composed by 866 different components

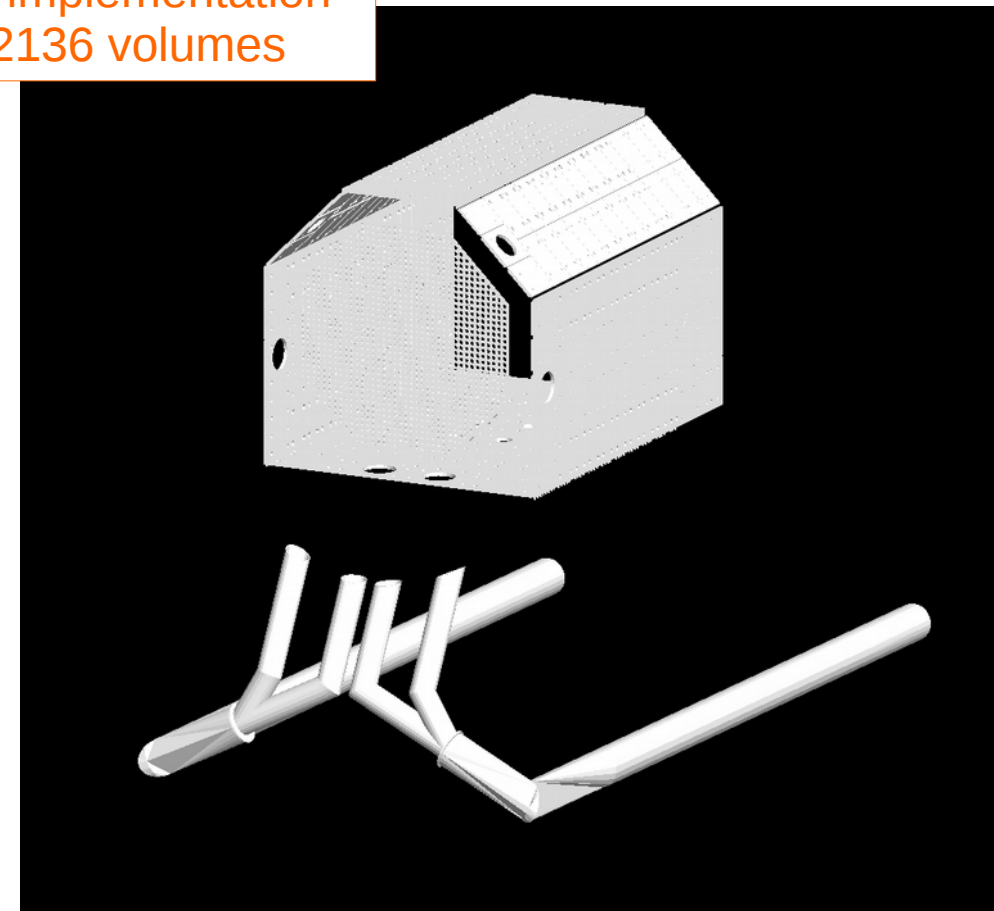
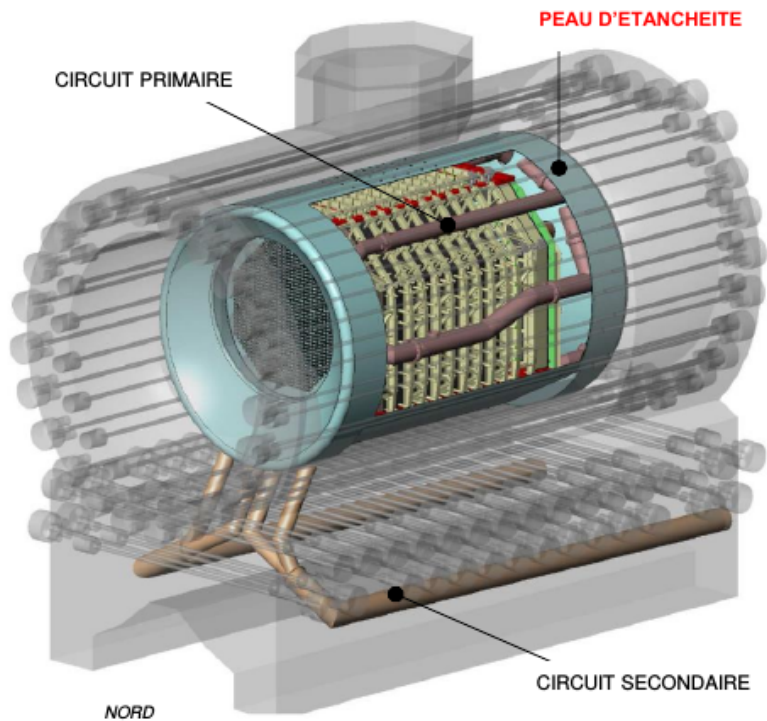
Towards high precision simulations: Implementation of geometries

From CAD designs

From objects 3D models: Topography, photo-grammetry...

G2-G3 reactors
CEA-Marcoule

G4 implementation
22136 volumes



CAD design composed by 866 different components

Summary and Conclusions

- **Atmospheric muons** is the main component of the air shower reaching the Earth's Surface.
 - They represent themselves, or by muon-induced events, one of the main background for particle physics
 - Reactor neutrino experiments
 - Going underground
 - Active vetoes
- **Double Chooz** has performed a full muon characterization combining data analysis and Monte Carlo simulations
 - Muon Rate and Flux, Angular distributions
 - Also annual modulation phenomenon → Validation of the theoretical models
- However, atmospheric muons represent an interesting radiation source utilisable for other applications
 - **Muon tomography** is a non-invasive exploration technique suitable for big objects
 - **Accurate simulations** could help to improve the sensitivity of this technique
 - Some preliminary studies have been already performed
 - More complete, versatile and precise framework is being implemented



Squeezing atmospheric muons

From neutrino physics to imaging applications

Héctor Gómez

IRFU / DPhN / LSN

hector.gomez@cea.fr

